Understanding the Role of Biological Time on the Morphology and Function of Microglia in the Prefrontal Cortex

Understanding the role of biological time on the morphology and function of microglia in the prefrontal cortex.

A Thesis Presented
by
STEPHANIE GOTTWALS

Submitted to the Graduate School of the
University of Massachusetts Amherst in partial fulfillment
of the requirements for the degree of
Master of Science

September 2024
Neuroscience and Behavior

Understanding the role of biological time on the morphology and function of microglia in the prefrontal cortex

A Master's Thesis Presented

by

Stephanie Gottwals
Spire ID: 32306240

Monday, August 26th, 2024

Committee Members:

Signed by:
Ilia Karatsoreos
Ilia Karatsoreos, Chair

DocuSigned by:
Karine Fenelon
Karine Fenelon, member

DocuSigned by:
David Moorman
David Moorman, member

DocuSigned by:
Heather N. Richardson
Heather Richardson
Graduate Program Director
Neuroscience and Behavior Program

Acknowledgements

I would like to express my deepest gratitude to my advisor, Ilia Karatsoreos whose guidance and encouragement pushed me to be my best while always allowing me to be myself. His support and belief in my potential made this journey not only possible but extremely enjoyable. I am also incredibly grateful to Gregory Pearson, who has been an invaluable mentor throughout this process. His insights, patience, and passion for the subject have been instrumental in shaping my work. I truly appreciate the time and effort he invested in helping me navigate the challenges of this research. A special thank you to my lab mate, and friend, Brennan, whose support and friendship kept me sane throughout this journey. Your humor, advice, and willingness to listen made the toughest moments manageable, and I'm grateful to have had you by my side. I am fortunate to have worked alongside such talented and supportive individuals in the Karatsoreos lab. The collaborative spirit, camaraderie, and shared dedication made our lab a place I looked forward to going to everyday. I would also be unable to complete this journey if it weren't for the support of my family and friends. To my family, friends, coached, and teammates, your unwavering love and support have been my foundation throughout this journey. Whether it was through words of encouragement, patience, or simply being there to listen, each of you has played a crucial role in helping me reach this point. I am deeply grateful for your unwavering belief in me and your constant support, even during my less-than-glamorous moments.

ABSTRACT

UNDERSTANDING THE ROLE OF BIOLOGIAL TIME ON THE MORPHOLOGY AND FUNCTION OF MICROGLIA IN THE PREFRONTAL CORTEX
SEPTEMBER 2024

STEPHANIE GOTTWALS, B.S., UNIVERSITY OF MASSACHUSETTS AMHERST
M.S., UNIVERSITY OF MASSACHUSETTS AMHERST

Directed by: Professor Ilia Karatsoreos

Circadian rhythms play an important role in maintaining the proper regulation of cognitive function and physiological processes. The importance of this system is highlighted when desynchronization of circadian rhythms occurs; however, the process by which these changes to brain and behavior remains unknown. Microglia cells are a possible mechanism for these changes because they are regulated by circadian rhythms and directly and indirectly influence synapses. In order to understand the role of time-of-day and perturbations of circadian rhythms on microglia morphology and function, a dual approach, using transcriptomics and multiplexed immunohistochemistry with imaging, was implemented. We observed an effect of time-of-day (ZT4 vs ZT16) on a range of functional pathways, including genes belonging to the “Activated Microglia” gene set, in the PFC of male and female mice. We demonstrated an increase in phagocytic capacity at ZT0 compared to ZT12. Under a T20 model of circadian desynchronization, a general upregulation in differentially expressed genes is visualized. When analyzing the combination of transcriptomics and morphological characteristics of microglia under T20 conditions, an overall more “activated” phenotype with higher phagocytic capacity was observed.

Table of Contents

List of Abbreviations

AD	Alzheimer's disease
AF	Autofluorescence
ANOVA	Analysis of variances
ASD	Autism spectrum disorder
Atp6v0eP	ATPase H+ transporting V0 subunit e Pseudogene
CCG	Core clock gene
CD	Circadian disruption
CD68	Cluster of differentiation 68
CT	Circadian time
CNS	Central nervous system
COX-2	Cyclooxygenase-2
Cry	Cryptochrome
CX3CL1	Fractalkine
C4A	Complement component 4A
DEG	Differentially expressed gene
ECD	Environmental circadian desynchronization
FN1	Fibronectin 1
GRP	Gastrin-releasing peptide
Iba1	Ionized calcium-binding adapter molecule
Il1r1	Interleukin 1 receptor type 1
Il6ra	Interleukin 6 receptor subunit alpha
LTD	Long-term depression
LTP	Long-term potentiation
MDD	Major depressive disorder
NDS	Normal donkey serum
NREM	Non-rapid eye movement
OB	Olfactory bulb
P2X	Purinergic receptor P2X
P2Y	Purinergic receptor P2Y
PAMPS	Pathogen-associated molecular patterns
PD	Parkinson's disease
PFC	Prefrontal cortex
PB	Phosphate buffer
PBS	Phosphate buffered saline
PBT	Phosphate buffer with Triton X-100
Per	Period
PFA	Paraformaldehyde
PS	Phosphatidylserine
Ptgs2	Prostaglandin-endoperoxide synthase 2
PSD95	Postsynaptic density protein 95
REM	Rapid eye movement
ROI	Region of interest
SCN	Suprachiasmatic nucleus
TOD	Time-of-day
TTFL	Transcriptional-translational feedback loop

T20	10-hour light: 10-hour dark cycle
T24	12-hour light: 12-hour dark cycle
VIP	Vasoactive intestinal polypeptide
XBP1	X-box binding protein 1
ZT	Zeitgeber time

List of Figures

1. Literature Review

1.1 Circadian Rhythms

Circadian rhythms are ubiquitous in biology, and a fundamental part of nearly all life on Earth. Circadian rhythms enable the synchronization of organisms to the day-night cycle caused by the 24-hour rotation of the Earth. In mammals, the daily changes in behavioral, mental, physical, and physiological functioning we observe are fundamentally driven by circadian rhythms. At their core, circadian rhythms are generated by molecular components at the cellular level in the brain "clock" in the suprachiasmatic nucleus (SCN) of the hypothalamus. The SCN then signals to other brain regions as well as peripheral tissues to generate local and systemic rhythms (Abe et al., 2002; Dibner et al., 2010). These rhythms are then synchronized through the interplay of entraining cues from the environment ("zeitgebers" or "time givers") and these molecular clocks.

The term "zeitgeber," (German for "time giver" or "synchronizer") refers to rhythmic environmental cues that can influence biological rhythms. While zeitgebers include rhythmic behaviors such as feeding, exercise, and other environmental factors such as temperature, light remains the primary zeitgeber for mammals (Ashton et al., 2022). To describe timing in relation to these external zeitgebers, the framework of Zeitgeber Time (ZT) is commonly used. In the case of light as an entrainment cue, under a 24-hour day, ZT0 represents the start of the light period, and ZT12 marks the beginning of the dark period in a 24-hour cycle. When an organism no longer has access to these zeitgebers and is "free-running" (or relying on its endogenous clock), circadian time (CT) is used to describe its location within a subjective period. Utilizing ZT enhances our understanding of how external conditions, particularly light, influence daily rhythms,

while CT helps understand the internal organization and persistence of rhythms without external cues. For decades, the location of the clock in mammals was unknown.

By the 1950s, it was widely accepted that biological rhythms were internally driven by a clock (or set of clocks), but the specific location of these internal "drivers" remained unclear (Patton & Hastings, 2018). It wasn't until heroic brain lesioning experiments that the SCN was discovered as the central circadian clock. These experiments revealed that damage to the SCN disrupted circadian rhythms, pinpointing it as a key regulator (Stephan & Zucker, 1972). Further studies demonstrated that the SCN, located in the anterior hypothalamus, receives external information through multiple pathways, including photic input from the retina via the retinohypothalamic tract (Patton & Hastings, 2018). Thus, the SCN coordinates various physiological and behavioral rhythms by synchronizing peripheral tissues with environmental light-dark cycles.

Research has further refined our understanding of SCN regulation by examining cell types that make up this brain region (Miller et al. 1996). Afferent inputs synapse on ventral "core" neurons that express vasoactive intestinal polypeptide (VIP) and gastrin-releasing peptide (GRP) (Patton & Hastings, 2018). The "shell" receives inputs from separate brain regions, such as the hippocampus, and intra-SCN projections from the ventral core (Leak et al., 1999). Efferents from the core and shell project to similar brain regions, such as the subparaventricular zone and dorsomedial hypothalamus (Yan et al., 2012). In many species, efferent connections with the pineal gland are imperative for rhythmic regulation of melatonin production (Borjigin et al., 2012). Other peripheral targets for generating and maintaining rhythms throughout the body include different glands, including the adrenal gland, with cortisol production being highly rhythmic.

These efferent projections underscore the SCN's role in coordinating systemic rhythms across various physiological processes. As alluded to above, central to this rhythmic coordination are the intrinsic molecular clocks present in virtually every cell, including those in the SCN. These molecular clocks operate through a transcriptional-translational feedback loop (TTFL) that modulates the rhythmic expression of core clock genes (CCGs), such as Bmal1, Period (Per), Clock, and Cryptochrome (Cry) (Ko & Takahashi, 2006). The interplay between these genes orchestrates the 24-hour oscillation that regulates circadian rhythms, influencing both cellular functions and broader physiological processes. A simplified explanation of the primary regulatory loop of the molecular clock is as follows: CLOCK and BMAL1 are transcription factors that heterodimerize, bind to DNA, and initiate transcription of E-Box genes, such as Per and Cry. PER and CRY proteins accumulate in the cytoplasm, form heterodimers, and translocate back into the nucleus (Ko & Takahashi, 2006). The PER:CRY heterodimer inhibits the activity of the CLOCK:BMAL1 complex, thus reducing their own transcription. The degradation of PER:CRY heterodimers over time relieves CLOCK:BMAL inhibition (Ko & Takahashi, 2006). This cycle, in tandem with another regulatory loop including retinoic acid-related orphan nuclear receptors Rev-erba and Rora, remarkably creates an approximately 24-hour oscillation. The oscillation of these core clock genes regulates the expression of numerous downstream genes, leading to rhythmic changes in cellular functions that, in turn, affect many physiological and cognitive processes.

1.1.2 Circadian Rhythms are Critical for Health

The importance of circadian rhythms in health is clear, though the mechanisms by which normal rhythms promote health and abnormal rhythms lead to pathology are not fully appreciated. The importance of circadian rhythms in mediating proper functioning is highlighted when circadian disruption occurs. Circadian disruption (CD) is a blanket (and sometimes overused) term encompassing various challenges to the endogenous 24-hour clock including circadian desynchronization, chronodisruption, circadian misalignment, and other disturbances (Vetter, 2018). Disruption of the biological clock may occur when exogenous cues conflict with each other (e.g., feeding and light schedules), when endogenous clocks become decoupled from each other (e.g., the central clock is out of phase with liver or other peripheral tissue clocks), or when the endogenous clock is unable to entrain to relevant cues (e.g., light cues are out of the entrainable range of endogenous SCN rhythms). The cause of these types of disruption includes inappropriate misalignment due to internal or environmental variables, including diseased states (Vetter, 2018).

Circadian disruption in humans has been linked to an increased risk and severity of neurological and psychiatric disorders. A bidirectional relationship between many of these disorders—specifically neurodegenerative and mood disorders—and circadian disruption has been elucidated in previous research. Importantly, circadian disruption is identified as both a symptom and a risk factor for many diseases (Abbott et al., 2018). Patients with neurodevelopmental disorders, such as autism spectrum disorder (ASD), often exhibit notable differences in circadian biomarkers, including disrupted melatonin and cortisol rhythms (Fishbein et al., 2021). In neurodegenerative diseases like

Parkinson's disease (PD) and Alzheimer's disease (AD), circadian rhythm misalignment is predictive of disease progression (Abbott et al., 2020). Psychiatric conditions, such as schizophrenia and major depressive disorder (MDD), are also associated with abnormalities in sleep cycles and cortisol rhythms (Walker et al., 2020). A striking example of circadian disruption affecting mood is seasonal affective disorder, where misalignment due to seasonal variations in light-dark periods contributes to the disorder (Fishbein et al., 2021). Given the widespread effects of circadian disruption on human health, understanding the role of circadian rhythms in normal functioning and the impact of circadian disruption on health is imperative.

1.1.3 Models of Circadian Disruption

To understand the role of circadian rhythms in human health, current research employs various chronic circadian disruption models in non-human animals. These models include genetic clock mutants, jet lag models, and altered day length models (e.g., T28, T20) (Vetter, 2018). Each model provides unique insights into how circadian disruptions impact biological processes.

Genetic clock mutant models, which carry mutations in core clock genes such as *Clock*, *Bmal1*, *Per*, and *Cry*, are particularly valuable for elucidating the molecular mechanisms of circadian regulation and their downstream behavioral and physiological effects. While common outcomes across these models include significant changes in feeding patterns and metabolic disruption (Arble et al., 2010), the specific phenotypes vary depending on the gene mutated. For example, *Clock* mutant mice display an extended free-running period and altered day-night activity and feeding patterns (Turek et

al., 2005). In contrast, *Bmal1* mutant mice exhibit a complete loss of rhythmicity under constant darkness conditions (Bunger et al., 2000).

Another approach to studying circadian disruption involves "jet lag" models, which simulate the effects of phase shifts on circadian rhythms. Jet lag in animals can be induced by single phase shifts or, in chronic jet lag, repetitive phase shifts. Typically, these phase shifts range from 6 to 14 hours. Studies using jet lag models have shown that different tissues re-entrain at varying time frames, leading to desynchronization of rhythms throughout the brain and body (Arble et al., 2011). Chronic jet lag studies have also demonstrated marked changes in immune activity and the risk of mortality in mice (Meng et al., 2023; Davidson et al., 2006). This model complements genetic studies by highlighting how acute changes in environmental cues can disrupt circadian synchronization.

Altered period length models further contribute to our understanding by providing an organism with a zeitgeber that falls outside the entrainable range of its intrinsic biological clock. An example of an altered period length model, referred to as LD20 or T20 in the literature, shortens the normal 24-hour day to 20 hours. Thus, animals spend 10 hours in the light and 10 hours in the dark. This method of environmental circadian desynchronization utilizes misalignment of internal (SCN) and external (light/dark) rhythms as a means of disruption. Since the 20-hour light cycle shift is out of the entrainable range, mice are unable to properly adjust to the novel 20-hour day. Results from this model have demonstrated changes in behavior, cognition, metabolism, and physiology in mice (Karatsoreos et al., 2011). Some general effects of the T20 model include disruption in the timing of core body temperature rhythms and accelerated weight

gain (Karatsoreos et al., 2011). In addition, previous work has demonstrated a significant effect of the T20 model on the distribution of REM and NREM sleep (Phillips et al., 2015; Hasan et al., 2018).

1.1.4 Effects of ECD on Brain and Behavior

Mice subjected to a chronic jetlag model of ECD, involving either phase advance or phase delay, demonstrate reduced hippocampal neurogenesis, decreased memory performance, and symptoms indicative of depression (Horsey et al., 2019). Transcriptional analysis of prefrontal cortex (PFC) tissues in this chronic jet lag model revealed an alteration of pathways linked with neurological disease (Siddique et al., 2022).

The T20 model has also demonstrated an effect on brain structure, function and behavior related to the murine PFC. For instance, investigators found reduced complexity of apical dendrites in PFC pyramidal neurons in layer 2/3 as a product of a decrease in the number of apical intersections, overall apical dendrite length, and apical branching (Karatsoreos et al., 2011). Moreover, intrinsic firing properties of these cells, such as the half width and amplitude of action potentials, were significantly altered by T20, resulting in an overall decrease in the excitability of layer 2/3 PFC pyramidal neurons (Roberts & Karatsoreos, 2023). Along with changes in the structure and function of PFC neurons, mice in T20 demonstrate PFC-dependent changes in cognitive function. Compared to T24 controls, mice subjected to T20 demonstrated an inability to modify their behavior to adapt to environmental changes in a modified water maze task (Karatsoreos et al., 2011). Given that the protocol for this water maze task was specifically selected to assess PFC

function, this finding highlights a decrease in cognitive flexibility generated by circadian desynchronization.

These findings underscore structural and subsequent electrical, functional, and behavioral consequences of the T20 model of circadian desynchronization. The cellular mechanisms by which T20 causes these changes remain unknown.

1.2 Potential Mechanism for T20 Changes

To narrow the potential cellular mechanisms that could be at play in the T20 model, we need to explore what is known about ways cells and circuits are remodeled, and if these effects might be impacted by T20. Neuronal connections and firing properties can be influenced by several mechanisms. Synaptic plasticity allows synapses to strengthen or weaken over time as a function of firing activity (Citri & Malenka, 2008). Long-term potentiation (LTP) and long-term depression (LTD) regulate synaptic strength by altering receptor number and activity and inducing structural changes (Citri & Malenka, 2008). Changes in intrinsic membrane properties, such as the expression of ion channels, also affect neuron excitability and firing patterns (Burke & Bender, 2019). Moreover, injury and disease states, such as epilepsy, traumatic brain injury, and neurological diseases, can disrupt neural circuits and damage neurons (Scharfman, 2007, Sato et al., 2001, Busche & Konnerth, 2016). Additionally, changes in cellular metabolism, such as variations in energy substrate availability or metabolic pathway alterations, impact neuron health, synaptic function, and overall neural activity (Magistretti & Allaman, 2015).

1.3 Microglia as mediators of synaptic and cellular plasticity

It is well understood that glial cell interactions are crucial in mediating the previously stated changes in neuronal connections and firing properties. Microglia, the brain's resident immune cells, not only respond to neural damage and pathogens but also play a vital role in monitoring and maintaining neural function under physiological conditions

Microglia are highly sensitive to their local microenvironment, enabling them to respond to invading pathogens and injuries under pathological conditions (Harry, 2016). This sensitivity also allows microglia to conduct homeostatic surveillance of the brain parenchyma under physiological states. Under such conditions, microglia mediate adult neurogenesis in the hippocampus, monitor the functional states of neurons, perform synaptic pruning, and phagocytose apoptotic cells (Cornell et al., 2021). Many roles of homeostatic microglia contribute to the modulation of the structural and functional states of neurons to optimize neuron-neuron communication (Paolicelli et al., 2011). Microglia are highly dynamic cells with the ability to assume a range of functional states. This key characteristic, coupled with the presence of an intrinsic molecular clock (Fonken et al., 2015; Hayashi et al., 2013), makes microglia a plausible candidate for explaining circadian-induced changes.

1.3.1 Microglial dynamics and their role in defining microglial function

The dynamic nature of microglia can be explained by their ability to assume different functional states that differ in motility, morphology, production of cytokines, and phagocytic activity.

To sense and react to the changing demands of the brain, microglia constantly extend and retract their processes in a process called motility (Nimmerjahn et al., 2005; Franco-Bocanegra et al., 2019). Two distinct brain state-dependent forms of motility are observed in microglia: baseline and directed motility. Baseline motility occurs under physiological states when microglia surveil their local environment, extending and retracting solely their processes in random, non-directed movements (Madry & Atwell, 2015). As microglia scan their individual territory, microglia maintain relatively high process speed, and each cell, in the cortex, can span a total of 60 μm (Nimmerjahn et al., 2005).

This differs from directed motility, also known as chemotaxis, which occurs under pathological conditions and involves the movement of both the processes and the cell soma (Franco-Bocanegra et al., 2019). In directed motility, microglia target the extension of processes toward sites of interest, such as injury or other cells in the central nervous system (CNS) (Madry & Atwell, 2015). A defining difference between the two mechanisms is the unilateral extension of processes observed in directed motility versus isotropic extension in baseline motility. Microglia engaged in directed motility selectively extend processes on the side of the cell closer to the site of CNS damage while retracting processes on the farther side. In contrast, microglia involved in baseline motility extend their processes in all directions (Madry & Atwell, 2015).

Similarities in these distinct types of motility can be seen in the consistent rearrangement of actin microfilaments to allow for changes in motility. To express motility and phagocytosis, microglia reorganize actin microfilaments into structures termed lamellipodia, filopodia, and uropods (Franco-Bocanegra et al., 2019). These

structures are made feasible by cross-linked actin networks consisting of actin polymers bound together by proteins (Franco-Bocanegra et al., 2019). In microglia, an integral and well-known cross-linking protein is the ionized calcium-binding adapter molecule (Iba1) (Oshawa et al., 2000). IBA1 is a commonly used marker for microglia cells because it is distributed throughout the cell body and processes, and labels microglia under both pathological and physiologic conditions.

Several receptors present on the cell surface of microglia work together to complete both directed and baseline motility. A family of receptors, known as purinergic receptors, mediate changes in directed motility by initiating a rapid response to ATP/ADP, UTP, and adenosine release in the local microenvironment (Haynes et al., 2006; Madry & Atwell, 2015). This family of receptors include ionotropic purinergic receptors P2X and metabotropic P2Y and P1 receptors (Illes et al., 2020). In response to the binding of these nucleotides and nucleosides to membrane-bound receptors, a range of physiological and intracellular signaling cascades are initiated (Madry & Atwell, 2015). In particular, the P2Y12 receptor is necessary for the process of directed motility, as demonstrated by the lack of chemotaxis in a P2Y12 receptor knockout-model (Haynes et al., 2006). Other families of receptors that play a role in modulating motility include adrenergic receptors and chemokine receptors, which will be discussed at length in later sections.

1.3.2 Morphological plasticity of microglia enables aspects of their function

Changes in microglia motility are often reflected by dynamic morphological changes. These morphological changes give rise to distinct functioning patterns which allow microglia to complete a wide range of functions. Historically, microglia

morphology was described as either “resting” or “activated”; microglia in the “resting” state assumed a ramified morphology, while “activated” microglia demonstrated amoeboid morphology (Vidal-Itriago et al., 2022). Due to an increased understanding of microglia under both physiological and pathological conditions, the two-state paradigm misconception has been challenged and expanded upon. The binary classification has been retired and a spectrum of activation states is now widely accepted. The ability for direct correlation between function and morphological phenotype highlights the need for more specific and well understood classifications of microglia morphology.

Microglia in the historically termed “activated” phenotype assume an amoeboid shape due to a retraction of processes and an increase in the size of the cell soma (Vidal-Itriago et al., 2022). This specific morphological change is often indicative of microglia responding to pathological challenges. Previous research has shown that microglia in this state are involved in high levels of directed motility and phagocytosis (Madry & Atwell, 2015; Vidal-Itriago et al., 2022). Most microglia cells assume an amoeboid morphology and express high levels of phagocytosis during development (Harry, 2014); during adulthood, these same characteristics can be observed in microglia responding to pathogens (Vidal-Itriago et al., 2022).

In addition to the canonical amoeboid response to pathogens, distinct rod-like and honeycomb phenotypes have been presented as alternate morphologies. The honeycomb morphology, demonstrated in mice as a response to compression injury, involves the retraction of most processes, with the remaining processes creating an overlapping network to protect the brain parenchyma (Roth et al., 2012). Rod-like morphology has been demonstrated in humans, non-human primates, and rodents in response to various

pathological processes, such as HIV encephalitis and epilepsy (Vidal-Itriago et al., 2022; Harbison et al., 2014). Microglia demonstrating rod-like morphology have long, narrow cell bodies and minimal, one-dimensional primary processes, with a total lack of secondary processes. Research suggests that this phenotype may offer neuroprotective effects to healthy neurons (Taylor et al., 2014).

Among the spectrum of activation states, ramified morphology is characteristic of "surveilling" microglia, which are highly branched with long processes (Vidal-Itriago et al., 2022). Microglia in this state demonstrate baseline motility with minimal movement of the cell body (Madry & Atwell, 2015). Ramified microglia are most commonly observed under physiological states surveilling brain parenchyma, contacting and interacting with neurons, and providing neuroprotection (Nimmerjahn et al., 2005; Vidal-Itriago et al., 2022).

Another morphological state characteristic of microglia under physiological conditions includes what is known as a "ball-and-chain" structure. This morphological state enables phagocytosis of small pieces of material by processes rather than the cell body (Sierra et el., 2010; Vidal-Itriago et al., 2022). This morphological state indicates that microglia involved in phagocytosis do not always assume an amoeboid shape. When assessing phagocytic activity of microglia, reliance on morphology alone may lead to misinterpretation.

1.3.3 Phagocytosis as an active state of microglial remodeling of the brain

Microglia are often actively involved in phagocytosis, whether it be by the cell soma under pathological conditions or by a combination of the cell soma and processes under physiological conditions (Vidal-Itriago et al., 2022). Under pathological

conditions, microglia engage in phagocytosis of neuronal debris, protein aggregates, apoptotic cells and other unwanted substances (Yang et al., 2009). In comparison, under physiological conditions, microglia can be observed phagocytosing synapses and spines to maintain energetically favorable and healthy neuronal connections (Cornell et al., 2021).

Similarly to macrophages, phagocytosis by microglia occurs in three key steps: (1) “find-me”, (2) “eat-me”, and (3) “digest-me”. To initiate phagocytosis, microglia must be recruited to a target of interest; this process may be random, as microglia surveilling brain tissue encounter chemotactic signals or may be directed via release of factors by apoptotic cells and debris. An example of a “find- me” signal is the release of ATP by apoptotic cells. As previously described, the P2Y12R senses and responds by initiating directed motility (Madry & Atwell, 2015). Surveilling microglia may come in contact with the soluble neuronal ligand CX3CL1 fractalkine which also exerts chemotactic effects on microglia (Pawelec et al., 2020).

Once they arrive at the target location, microglia employ an array of receptors (as discussed above) to interpret "eat-me" signals, which indicate that a cell needs to be phagocytosed and removed, and "don't eat-me" signals, which suggest that a cell is healthy and should be left alone. Microglia express receptors specialized for securing themselves to the target cell and others specific to internalization (Sierra et al., 20). Different receptors are employed under varying conditions. “Don’t eat-me” signals, such as CD47 and CD200, inhibit the ability of microglia phagocytosis. A common example of a membrane-anchored “eat-me” signal is phosphatidylserine (PS), a marker for the selective engulfment of apoptotic cells (Wang et al., 2021). PS may affect microglia

function both directly and indirectly; receptors involved in a direct effect include TREM2 and TIM4 while TAM receptors are indirectly involved (Ma et al., 2022). Another family of microglia receptors specialize in the detection of pathogen-associated molecular patterns (PAMPS) and this includes immunoglobulin, scavenger, and toll-like receptor families (Sierra et al., 2013). Research has highlighted the role of fraktaline, soluble opsins, and other signaling factors in the engulfment and refinement of synapses.

When the "eat-me" pathway is activated, a phagocytic cup forms due to alterations in the actin cytoskeleton and the cell membrane of microglia (Sierra et al., 2013). Closing the phagocytic cup creates a phagosome that engulfs the tissue of interest. As these phagosomes mature and become more acidic, they fuse with lysosomes containing digestive enzymes to create phagolysosomes (Wang et al., 2021). Hydrolases and proton pumps can be found within phagolysosomes, helping to create the appropriate acidic environment for digestion (Sierra et al., 2013). These three key steps allow microglia to select and consume the correct target and successfully break down unwanted material.

1.3.4 Neuron-Microglia interactions as a key to understanding remodeling

To understand microglia as a potential mechanism through which ECD influences neuronal structure and function, it is important to explore interactions between neurons and microglia. Neuron-microglia interactions were initially discovered through observing the baseline motility of surveilling microglia, as well as their expression of neuronal signaling factor receptors. These traits, coupled with the cell's phagocytic capacity, implicated microglia in research on structural and functional changes in neurons, such as synaptic remodeling and neurogenesis.

Previous studies have shown that microglia can detect neuronal activity through a variety of membrane receptors responsive to neurotransmitters, neuromodulators, neurohormones, and other neuron-related signaling factors (Ketteman et al., 2011). Two examples of these receptors found on the microglia membrane include AMPA and adrenergic receptors (Ketteman et al., 2011). When AMPA receptor agonist kainate is applied to cultured microglia, excitation in terms of actin rearrangement and morphological plasticity is observed (Christensen et al., 2006). More specifically, following bath application of glutamate, microglia target processes toward surrounding neuronal elements (Eyo et al., 2014). β2-adrenergic receptors are highly expressed on microglia and application of norepinephrine induces increased process retraction and decreased ramification, indicative of an amoeboid phenotype (Gynovea & Traynelis, 2013). These findings confirm that microglia can sense synaptic activity.

A more concrete relationship between microglia and neurons has been demonstrated by visualization of microglia actively engaged in contacting pre- and postsynaptic elements. *In vivo* two-photon microscopy in the somatosensory cortex of mice showed that microglia briefly and specifically contact pre- and postsynaptic structures (Wake et al., 2009). This study also demonstrated an activity-driven mechanism for microglial contact with synapses, where an increase in basal neuronal activity promotes microglial interaction with neurons (Wake et al., 2009), substantiating that microglia sense synaptic activity. Research on synaptic pruning by microglia, using ex vivo imaging, has shown that microglia engulf and internalize synaptic proteins, such as synaptophysin and PSD-95 (Choudhury et al., 2019; Paolicelli et al., 2011). Not only has research demonstrated that microglia are involved in synaptic pruning but has shown

that pruning by microglia is necessary for normal neuronal function (Paolicelli et al., 2011). Mice lacking the CX3CR1 receptor, a transmembrane G-protein coupled receptor, expressed by microglia, for the fractalkine CX3CL1, expressed by neurons, demonstrate significantly higher dendritic spine densities and drastic changes in the electrophysiological properties of neurons, thus affecting overall neural circuitry (Paolicelli et al., 2011).

1.3.5 Microglia heterogeneity is defined by context, time and space

Due to the diversity of brain tissue and the ability of microglia to respond to their specific environments, microglia exhibit phenotypic differences in relation to contextual, temporal, and spatial cues. Consequently, the morphological and functional states of microglia are highly heterogeneous. Contextual differences may include previously described changes in brain tissue, such as brain injury or infection.

Temporal differences in phenotype on the scale of development are observed as a function of age—drastic changes in phenotype are observed between prenatal, postnatal and microglia in models of aging (Harry, 2013). For example, aged microglia express higher levels of activation markers, such as CD45, when compared to early postnatal microglia (Antignano et al., 2023). Time on the circadian scale is also known to affect particular aspects of microglia function, such as motility and immune response (Hayashi et al., 2013; Fonken et al., 2015).

To further explore temporal dynamics, it's important to consider even shorter time scales—such as those on the order of minutes or hours. Recent studies have documented notable changes in microglial motility and process length within these timeframes. For example, live imaging of freely behaving mice revealed that microglial processes extend

and retract within a 30-minute wake period, with an average motility of approximately 1.4 microns per minute (Gu et al., 2023). Similarly, this approach has demonstrated significant variations in microglial characteristics, such as process length, motility, and volume, between different sleep-wake states (Gu et al., 2023).

In relation to spatial cues, previous work has demonstrated tissue-specific diversity in microglial marker expression and microglial density (Masuda et al., 2020). Significantly higher expression of CD68 and IL-1β is observed in the olfactory bulb compared to regions such as the hippocampus and substantia nigra indicating brain-region-specific gene expression profiles (Doorn et al., 2015). Studies have also demonstrated regional heterogeneity in the microglial transcriptome, particularly between the cerebral cortex and the hippocampus (Grabert et al., 2016). These findings reveal regional differences in the ability of microglia to initiate and carry out effective immune responses (Grabert et al., 2016). Different brain regions may require functional variations in microglia to carry out region-specific tasks. As previously described, microglia respond to their local microenvironment and thus this environment shapes microglial activity. Differences in neuronal subtype, neural activity, and neurotransmitter levels may contribute to this regional variation (Grabert et al., 2016).

1.4 Digging deeper: Microglia around the clock

It is well understood that microglia express core clock genes rhythmically (Fonken et al., 2015; Hayashi et al., 2013). As noted above, microglia demonstrate rhythmic changes on the circadian time scale. For example, cortical microglia demonstrate diurnal morphological changes driven by expression of the PY2R12 receptor under healthy conditions (Hayashi et al., 2013). More specifically, an increase in the

number of branches and the total length of microglia processes is increased during the dark phase (ZT14 and ZT18) when compared to the light (ZT4 and ZT6), a phenomenon ablated in CLOCK mutant mice (Hayashi et al., 2013). Rhythmicity in microglia morphology and expression of microglia-specific markers has also been demonstrated in the prefrontal cortex of rats. Diurnal activation of microglia is evidenced by increased expression of markers such as CD45, CD68, and CD11b at the onset of the light phase (ZT0) (Choudhury et al., 2019). As evidenced by the time-of-day effects on microglia in the prefrontal cortex of rats and the cortex of mice, species and brain regions may demonstrate morphological, transcriptional, and activational differences in microglia across the parenchyma. These time-of-day effects are of interest as they may affect the ability of microglia in specific regions of the brain to surveille neural tissue, interact with neurons, and respond to brain injury and immune challenges differently.

Premise of Current Work

Previous work from our lab has demonstrated that chronic circadian disruption, specifically a T20 model of desynchronization, results in significant changes to neuronal structure and cognitive capability. The mechanisms underlying the impact of chronic circadian disruption on the brain is unknown. Microglia provide a mechanism by which these changes may occur. We hypothesize that characteristics of microglia are time of day-dependent and that the T20 model will disturb homeostatic microglia morphology and increase phagocytic capacity in the prefrontal cortex. Thus, assessing the effect of time-of-day and perturbations of circadian rhythm on microglia morphology and function may help us towards understanding the mechanisms underlying T20 changes.

2. Circadian Rhythms Mediate the Morphology and Function of Microglia in the PFC of Male and Female Mice.

2.1 Introduction

Circadian rhythms are widespread in biology and essential for almost all life on Earth. Circadian rhythms facilitate the synchronization of physiological processes with the day-night cycle, which seems important for optimal function. In mammals, these rhythms drive daily variations in behavior, cognition, physical activity, and physiological processes. The mammalian brain "clock" is located in the suprachiasmatic nucleus (SCN) of the hypothalamus, where rhythms at the cellular and tissue level are driven by a molecular mechanism that generates circadian rhythms at the cellular level (Abe et al., 2002; Dibner et al., 2010). Circadian synchronization with the environment is regulated by the interplay between the function of the SCN and changes in environmental cues known as "zeitgebers", the most important of which is light (at least in mammals). The SCN receives and synchronizes brain and peripheral circadian oscillators to these zeitgeber cues (Hastings et al., 2003).

Like many fundamental aspects of physiology, the role of circadian rhythms is most evident when they do not operate correctly. With regards to circadian rhythms, this is most obvious when circadian disruption (CD) occurs. This term refers to any disturbance to the endogenous 24-hour clock. CD can result from conflicting zeitgebers, decoupling of endogenous clocks, or zeitgebers falling outside the entrainable range of the intrinsic biological clock. Given that the SCN synchronizes peripheral oscillators, circadian disruption leads to widespread dysregulation of rhythmic processes across tissues (Hastings et al., 2003). Studies of various animal models, including genetic clock

mutants, jet lag simulations, and altered day length scenarios, reveal the extensive and pervasive impacts of circadian disruption throughout the brain and body.

When the internal clock is unable to synchronize with external stimuli, a cascade of physiological and behavioral issues may arise. General effects often manifest as misalignment of activity and feeding schedules, metabolic disturbances, and altered hormone secretion (Arble et al., 2010; Gnocchi & Bruscalupi, 2017). The SCN also regulates various neural processes. Disruption in circadian rhythms can lead to significant changes in brain structure and function. For example, CD has been linked to alterations in synaptic plasticity in murine models (Barnes et al., 1977). Structural changes in the complexity of neurons in layer 2/3 of the PFC have also been shown (Karatsoreos, 2011). These changes underscore the profound influence of circadian rhythms on brain health, though the mechanisms driving these alterations remain unknown.

A possible mechanism by which cognitive and neuronal changes occur under chronic circadian disruption is through alterations in microglial function. Microglia play a pivotal role in responding to pathogens and injuries under pathological conditions (Harry, 2016), but under physiological states, they are crucial for maintaining homeostasis in the brain parenchyma through constant surveillance (Vidal-Itriago et al., 2022). Surveillant microglia are involved in several key processes, including mediation of adult neurogenesis in the hippocampus, monitoring the functional states of neurons, synaptic pruning, and phagocytosis of apoptotic cells (Cornell et al., 2021). These homeostatic roles are essential for modulating the structural and functional states of neurons, working to augment neuron-neuron communication (Paolicelli et al., 2011). The dynamic nature of microglia, combined with their intrinsic molecular clock (Fonken et al., 2015; Hayashi

et al., 2013), positions them as likely players in the brain's response to circadian disruption.

In the present study, we evaluate the influence of time-of-day and perturbations of circadian rhythm on prefrontal cortex tissue and the morphological states of microglia within this region in male and female mice. We developed a novel, unsupervised microglia detection method for image analysis, which can be applied to large datasets. We found a time-of-day and sex difference in the overall transcriptomic landscape of the PFC between ZT4 and ZT16, as well as a time-of-day difference in the phagocytic capacity of microglia. Under T20 environmental circadian desynchronization conditions, we found an upregulation of neuropathology-related genes in the PFC of male mice. Additionally, this model revealed changes in microglial phagocytic capacity and cell structure, indicating a shift toward more “activated” microglial phenotypes.

2.2 Methods

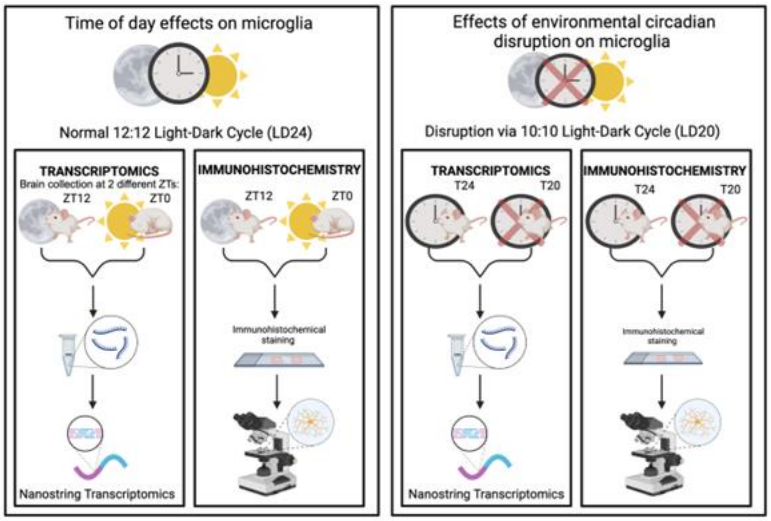

Figure 1. Depiction of general experimental design.

2.2.1 Experimental Design

To assess the role of time of day and circadian rhythm perturbations on the function and morphology of microglia, a dual approach using transcriptomics and immunohistochemistry was employed. Time-of-day effects on microglia were evaluated by comparing characteristics at multiple times of day under a normal 12-hour light: 12-hour dark (T24) cycle. Environmental circadian disruption (ECD) was induced through a 10-hour light: 10-hour dark (T20) cycle, and both morphological and functional characteristics were assessed.

2.2.2 Animals

Animals used in time-of-day experiments included male and female wild-type C57BL6N mice (Charles River) received at 8 weeks of age. Mice were split into four groups (N=16). They were then double housed in LD24 until 12-13 weeks of age with *ad libitum* access to food and water. Animals used in *Environmental Circadian Desynchronization (ECD)* experiments included male and female wild-type C57BL6N mice received at 6 weeks of age. They were double housed in LD24 until 7 weeks of age. They were divided into 4 groups (N=24) and subjected to either T20 or T24 until 12-13 weeks of age with *ad libitum* access to food and water. Light levels were monitored with a HOBO detector to ensure the correct lighting schedule was followed. All work with vertebrate animals was approved by the UMass Amherst IACUC.

2.2.3 Euthanasia and Tissue Collections

For time-of-day and ECD gene analysis experiments, brains were collected from mice at 12-13 weeks of age via live decapitation at two times of day (ZT4 and ZT16). Mice used in morphological experiments underwent intracardial perfusion and tissue collection at

12-13 weeks of age. Mice were anesthetized via intraperitoneal injection with a mixture of ketamine hydrochloride and xylazine. Perfusions were completed with ice-cold PBS and subsequent perfusion with 4% PFA Brains were collected and post-fixed in 4% PFA for 24 hours, followed by immersion in 20% sucrose for 24 hours and 30% sucrose for another 24 hours. Post-fixed brains were stored at -80°C until sectioning. Coronal sections (20 µm thick) were collected from the olfactory bulb to the cerebellum (CM3050 S, Leica, Germany). Slices were mounted directly on glass microscope slides.

2.2.4 RNA Extraction

Microdissections were performed to obtain tissue for gene analysis. Brains were mounted and sectioned at 50 µm increments (CM3050 S, Leica, Germany) until the PFC was visualized (Bregma 2.545 mm). 1 mm deep micropunches (Item # 18035-01, Fine Science Tools) were collected from both hemispheres and stored in RLT + DTT.
RNA extractions were performed on microdissected tissue from the PFC using Qiagen's RNEasy Micro kit (Kit # 74004, Kit lot # 166034493). RNA quantification was completed using a Thermo Fisher Scientific Qubit fluorometer. The purity of extracted RNA was analyzed using Nanodrop spectrophotometry methods; the A260/280 and A260/230 ratios were used to determine protein and organic contamination, respectively. Purified total RNA was stored at -80 °C until required for gene analysis.

2.2.5 Nanostring Transcriptomics

Purified total RNA from the PFC was analyzed using Nanostring's nCounter technology (CPTC Genomics Core, UMass Boston). The nCounter neuropathology panel was used to assess 760 transcripts across multiple times of day and under both T20 and T24

conditions. The ROSALIND platform was used for nCounter analysis which included normalization, gene set analysis, and differential expression analysis.

2.2.6 Immunohistochemistry

Pre-staining Photobleaching Technique: To eliminate the confound of variable levels of intrinsic fluorescence in brain tissue (Stillman et al., 2023), photobleaching was completed post-sectioning. A photobleaching unit was constructed following a combination of two previously described protocols (Stillman et al., 2023; Sun et al., 2017). To create a cost-effective photobleaching unit, a large bin was lined with aluminum foil to produce a reflective container. A 36 W blue LED light bulb (HIGHGROW) was attached to a hanging lantern light lamp cord (Simple Deluxe Store) to hang the LED 3 inches above the incubating slides. A clear wash bin, used for immunohistochemistry washing steps, was filled with 0.1 M phosphate buffer (PB). To cover the top of the bin, an aluminum foil-wrapped lid was created which allowed room for the LED. Prior to photobleaching, an ImmEdge pen was used to create a hydrophobic barrier around tissue. Slides were left to incubate in the apparatus for a total of 48 hours in a 4 °C cold room. Slides incubated in PB without photobleaching steps were compared to slides incubated in PB and photobleached. The autofluorescence seen in the control sides was drastically quenched in the photobleached slides. This process did not interfere with subsequent staining steps.

Triple-Label Immunohistochemistry: Slides were blocked in a mixture of 2% normal donkey serum (NDS) (Jackson Immuno, 156021) and 0.1 M PB with 0.1% Triton X-100 (PBT) for 30 minutes. This mixture was removed, and slides were incubated in rabbit anti-IBA1 primary (1:1000, Fuji, Wako, Lot # 019-19741) and rat anti-CD68 (1:1000,

BioRad, Batch # 153593) for 48 hours at 4 °C. Concentration of primary was selected from test slides with concentrations of 1:200, 1:500, and 1:1000; the 1:1000 concentration was sufficient for both primaries. After incubation with primary, slides were washed for a total of 15 minutes (3 X 5min) with 0.1 M PBT. Slides were incubated in secondary antibodies - AlexaFluor 488 donkey anti-rabbit (1:200, JacksonImmuno, Lot # 124881) and AlexaFluor 647 donkey anti-rat (1:200, JacksonImmuno, Lot # 168360) - for one hour. These concentrations were selected from test slides with concentrations of 1:100 and 1:200 (the recommended concentration); the 1:200 concentration was sufficient for both secondaries. Subsequently, slides were washed in PBS for 15 minutes. Fluoromount-G mounting medium with DapI was used to mount slides.

Immunohistochemical Controls: Two control slides were tested to ensure that secondary antibodies did not bind nonspecifically to inappropriate primary antibodies or to tissue. The first included IBA1 primary and secondary with CD68 secondary to assess nonspecific binding of CD68. The second control assessed nonspecific binding of IBA1 secondary by staining with CD68 primary, CD68 secondary, Iba1 secondary. These steps ensure that the signal visualized is specific to the target antigens.

2.2.7 Imaging and Image Analysis

Slides were imaged using the fully automated TissueFAXS SL cytometry microscope. ZStacks (20 microns thick) of large regions were collected at 40x magnification with a 0.5-micron step size.

Images were exported from the TissueGnostics software and converted into appropriate files for analysis using ImageJ (Version1.54j, Fiji, Japan). Images were analyzed using NIS Elements software (Version 6.02, Nikon Instruments Inc., Japan) utilizing a batch

GA3 (General Analysis 3) recipe to automate and standardize the post-imaging analysis process across many images. More information regarding the imaging to analysis pipeline is described in supplemental figures and general discussion.

2.2.8 Statistical Analysis

For analysis of transcriptomics data in ROSALIND, fold change and p-values were calculated using a simplified negative binomial model. Results were deemed significant with a p-value < 0.05 and fold-change > |1.2|. Statistical analyses were performed using one-way analysis of variances (ANOVA) with a post-hoc Tukey's test, two-way ANOVA with repeated measurements, or chi-squared test in RStudio Software (Version 2023.03.1+446, Posit Software). Differences were deemed significant at $p < 0.05$.

2.3 Results

Many aspects of PFC function and PFC-dependent behaviors are affected by time-of-day (TOD) (Baltazar et al., 2013; Karatsoreos et al., 2011). In addition, disruption of the circadian clock leads to changes in both the structure and physiological function of PFC neurons (Karatsoreos et al., 2011; Roberts & Karatsoreos, 2023). We first wanted to understand how time-of-day affected the transcriptomic landscape of the PFC under steady state conditions. We used a Nanostring nCounter Mouse neuropathology panel - including 760 target mRNA transcripts - to probe changes in several different gene pathways in male and female mice at ZT4 and ZT16.

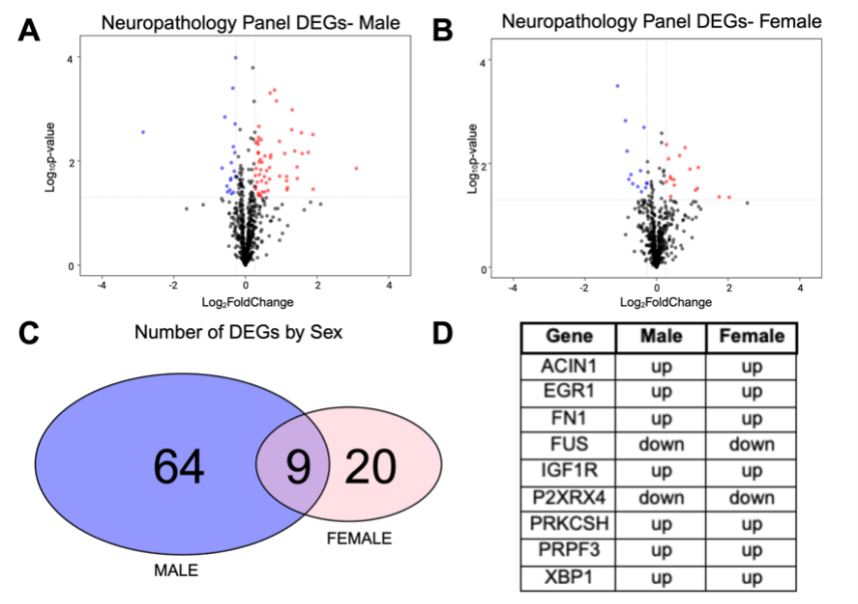

Gene	Male	Female
ACIN1	up	up
EGR1	up	up
FN1	up	up
FUS	down	down
IGF1R	up	up
P2XRX4	down	down
PRKCSH	up	up
PRPF3	up	up
XBP1	up	up

Figure 2: Time-of-day affects the expression of mRNA transcripts related to neuropathology, with a more pronounced effect observed in male mice compared to female mice. (A) Volcano plot depicting differential gene expression in the nCounter Mouse Neuropathology Panel at ZT16 compared to ZT4 in male (n= 73 differentially expressed/760 total genes, 10%) and (B) female mice (n= 29 differentially expressed/ 760 total genes, 4%). (C) Venn Diagram illustrating the overlap in differentially expressed genes between male and female mice. Each circle represents the number of DEGs in either male or female mice, with the overlapping region indicating genes that are differentially expressed in both sexes. (D) Direction of regulation in males and females of shared genes. n= 3 mice per group. Significance reported when $p < 0.05$ and Fold Change > Log2|1.2|.

In male mice, a total of 73 out of 760 genes included in the neuropathology panel were differentially expressed at ZT16 when compared to ZT4 (Fig. 2A). In the PFC of female mice, a total of 29 genes were differentially expressed at ZT16 when compared to ZT4 (Fig 2B). These results demonstrate a time-of-day difference in the expression of about 15% of genes in this panel (when combining male and female data). Among the differentially expressed genes (DEGs) observed in males and females, the majority (84/93, 90%) appear to be sex-specific, with only nine DEGs shared between the two (Fig. 2C & D).

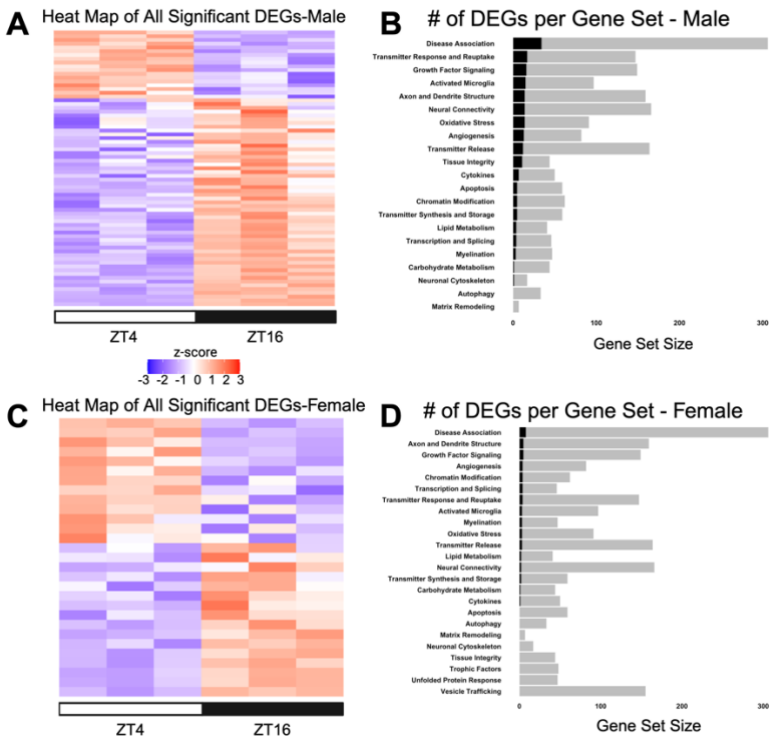

Figure 3. Time-of-day influences a range of functional pathways in the prefrontal cortex of male and female mice. (A) Heatmap displaying all significantly differentially expressed genes in the nCounter Mouse Neuropathology Panel in male and (C) female mice. (B) Bar graph showing the number of genes associated with each nCounter Mouse Neuropathology Panel Gene Set and the number of differentially expressed genes within each annotation in male and (D) female mice. The total number of genes per annotation is represented by the full bar height, while the shaded portion indicates the subset of differentially expressed genes. n=3 mice per group. Significance reported when $p < 0.05$ and Fold Change > Log2|1.2|.

In male mice, a majority (55/73, 75%) of DEGs were significantly upregulated at ZT16 when compared to ZT4 (Fig. 3A). The nCounter Mouse Neuropathology Panel includes 24 pathway annotations that associate DEGs with relevant biological pathways. The top five gene sets with the highest numbers of DEGs in male mice are “Disease Association,” “Transmitter Response and Reuptake,” “Growth Factor Signaling,” “Activated Microglia” and “Axon and Dendrite Structure” (Fig. 3B).

In female mice, greater variability was observed in the direction of regulation of the differentially expressed genes at two contrasting times of the day (Fig. 3C). Out of the

29 DEGs, we found 16 mRNA transcripts to be upregulated (55%) and 13 to be downregulated (45%) at ZT16 (Fig. 3C). Similar to our results in males, three of the top five gene sets with the highest numbers of DEGs in female mice include “Disease Association, “Axon and Dendrite Structure” and “Growth Factor Signaling”. (Fig. 1D). The two other gene sets with the highest number of DEGs are “Angiogenesis” and “Chromatin Modification” (Fig. 1D).

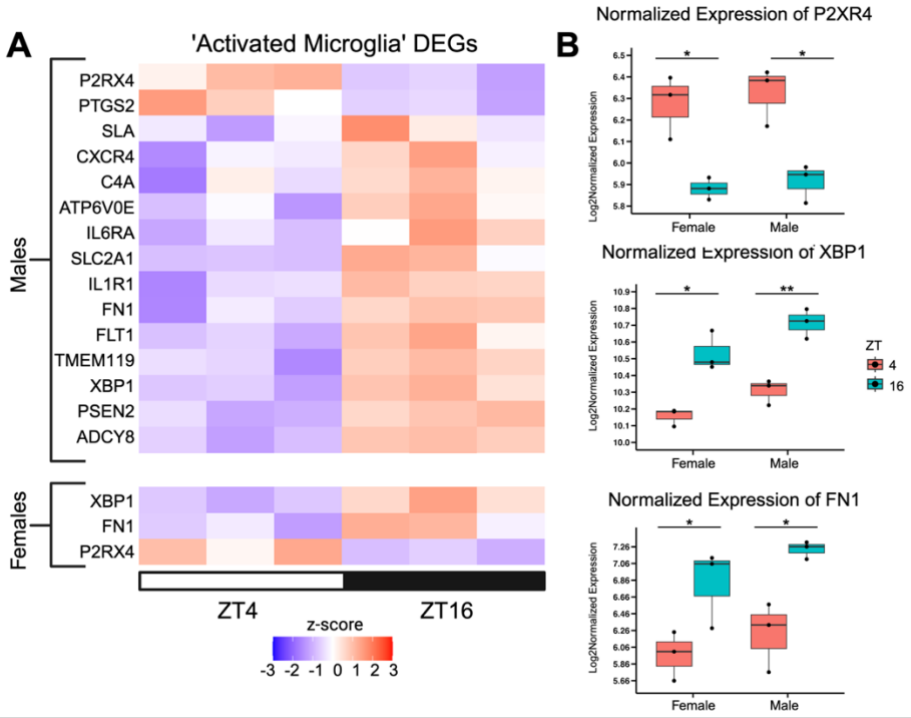

Figure 4. An upregulation of ‘Activated Microglia’ mRNA transcript expression is observed at ZT16 in male mice. (A) Heatmap of significantly differentially expressed genes in the Activated Microglia Gene Set in male mice and female mice (B) Normalized expression of the three genes - *P2XR4, XBP1*, and *FN1* - similarly differentially expressed in male and female mice. n= 3 mice per group, *p < 0.05, **p < 0.01.

Given the importance of microglia in the mediation of many of the pathways that showed differential expression, we further explored this pathway. In males, of the 73 DEGs in the nCounter Mouse Neuropathology Panel, a total of 15 belonged to the “Activated Microglia” gene set (Fig. 4A). Of these microglia-related DEGs, we found 13

to be upregulated at ZT16 (Fig. 4A). The microglia-related DEGs upregulated at ZT16 are involved in a range of microglia characteristics, including phagosome acidification - ATPase H+ transporting V0 subunit e Pseudogene (*Atp6v0eP*) (Fairely et al., 2023), response to cytokine signaling - Interleukin 6 Receptor Subunit Alpha (*Il6ra*) and Interleukin 1 Receptor Type 1 (*Il1r1*) (Burton et al., 2013; Basu et al., 2004), and selective elimination of synapses – Complement Component 4A (*C4a*) (Yilmaz et al., 2021) (Fig. 4A). The two DEGs found to be upregulated at ZT4 compared to ZT16 are Prostaglandin-Endoperoxide Synthase 2 *(Ptgs*2), commonly known as Cyclooxygenase-2 (COX-2), and Purinergic Receptor P2X 4 (*P2rx4)* (Fig. 4A). These results suggest an increase in microglia activity during the active phase in male mice.

In female mice, three out of the 29 DEGs were categorized under the 'Activated Microglia' gene set (Fig. 4A); these three genes are similarly differentially expressed in male mice (Fig 4B). The expression of *P2xr4* was significantly increased at ZT4 in both females (simplified negative binomial model, $p = 0.028$) and males ($p = 0.03$). Additionally, at ZT16, a significant increase in the expression of Fibronectin 1 (*FN1*) (females, $p = 0.03$; males, $p = 0.02$) and X-box Binding Protein 1 (*XBP1*) (females, $p = 0.018$; males, $p = 0.009$) was observed (Figure 4B). These results indicate that, at least between ZT4 and ZT16, there is less time-of-day difference in microglia activity in female mice compared to male mice.

Given that microglia are implicated in our transcriptomic findings, we wanted to further ascertain how they might be regulated in the PFC at different times of day. To accomplish this, we used triple label immunohistochemistry coupled with a custom-made

image analysis program to investigate how time-of-day impacts aspects of microglial structure and function in the PFC.

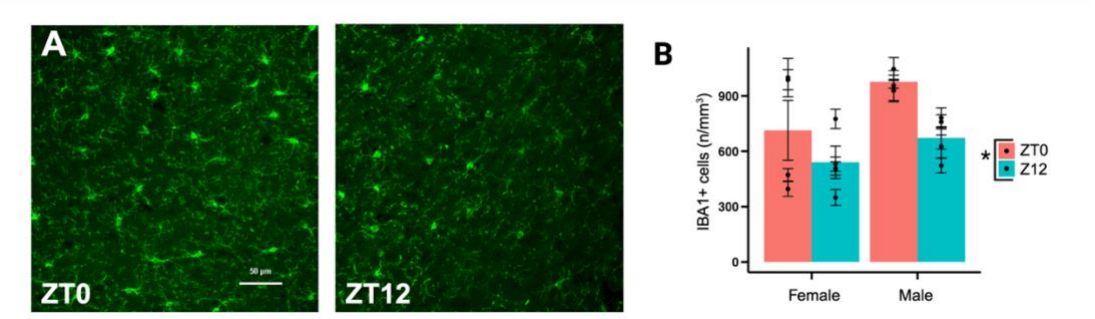

Figure 5. Diurnal variation in the number of IBA1+ cells in the prefrontal cortex. (A) Representative 40x images from male mice at ZT0 and ZT12. (B) Quantification of IBA1+ cell counts in male and female mice at ZT0 and ZT12. n= 3-4 mice per group. All data show mean ± SEM, *p < 0.05. Magnification bar = 50 µm.

Although limited in scope, previous studies have demonstrated that the time of day influences specific morphological characteristics of microglia, such as branching in the somatosensory cortex of male mice and soma size and Cd11b immunoreactivity in the prefrontal cortex of male rats (Hayashi et al., 2013; Choudhury et al., 2019). To analyze a comprehensive set of microglia characteristics in large tissue samples, we developed a user-friendly, unsupervised detection method for image analysis (Supplemental Methods, Fig. 3). On average, 2,400 microglia cells were detected per group (650 microglia cells per animal). Using this method, we observed a significant main effect of time of day, with an increase in the number of IBA1+ cells in the PFC at ZT0 compared to ZT12 (Two-way ANOVA, $F_{1,11}$= 4.851, p = 0.049) (Fig. 5B). We did not observe a main effect of sex (Two-way ANOVA, $F_{1,11}$= 2.757, p = 0.125), or an interaction (Two-way ANOVA, $F_{1,11}$= 0.380, p = 0.550).

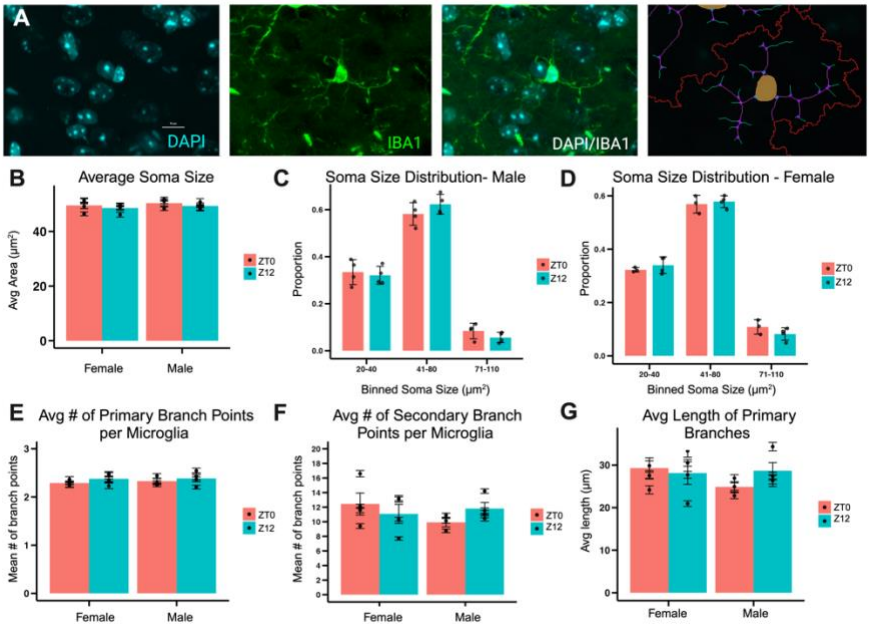

Figure 6. Time-of-day does not mediate changes in microglia complexity. (A) Representative image demonstrating colocalization of IBA1 with DAPI to identify cell soma (orange). Primary branches (purple) and secondary branches (turquoise) are also visualized. (B) Average soma size of microglia cells at ZT0 an ZT2 in male and female mice. (C) Proportions of microglia soma sizes within size bins by ZT in male and (D)female mice. (E) Average number of primary branch points per microglia cell soma in males and females at ZT0 and ZT12. (E) Average number of secondary branch points per microglia cell soma in males and females at ZT0 and ZT12. (F) Average length of primary branch points in males and females at ZT0 and ZT12. (G) Average length of secondary branch points in males and females at ZT0 and ZT12. n = 3-4 mice per group. All data show mean ± SEM, *p < 0.05, **p < 0.01. Magnification bar = 10 µm.

To characterize the morphology of microglia cells, the size of the soma, number of primary and secondary branch points, and the length of primary and secondary branches were characterized. Microglia cell bodies were identified by IBA1 and DAPI colocalization and further filtered by shape, fluorescence intensity, and area to reduce the artifacts of either the staining or imaging processes (Fig. 6A). We did not observe a main effect of time of day (Two-way ANOVA, $F_{1,11}$= 1.814, p = 0.205), or sex (Two-way ANOVA, $F_{1,11}$= 0.786, p = 0.394) in the average soma size, and there was no interaction (Two-way ANOVA, $F_{1,11}$= 0.002 p = 0.967) (Fig. 6B). However, we observed a skewed

distribution in soma areas across animals (Supplemental Fig. 1), which led us to further parse the data into smaller bins to categorize the different types of microglial cell bodies (Fig. 6C & D). To determine the association between ZT and soma size bin, we performed a chi-squared test of independence. The results revealed a significant effect of ZT on the distribution of soma size bins in female mice ($\chi^2(2) = 27.105$, $p < 0.0001$). A similar difference was observed in males ($\chi^2(2) = 14.833$, $p = 0.0006$). This indicates that the proportion of soma size bins varies significantly across different ZTs, suggesting a time-of-day effect on soma size distribution. The soma size bins were further analyzed using independent t-tests in which we found no significant interaction between soma size groupings and ZT in females (t-test: 20-40; t= 0.411, $p = 0.697$, 41-80; t= -1.289, p=0.698, 81-110; t=1.395, p= 0.212), or males (t-test: 20-40; t= -1.064, $p = 0.354$, 41-80; t= -0.423, p=0.698, 81-110; t=1.3982, p= 0.221) Although no significant interaction was observed between bin size and ZT, the presence of distinct distribution patterns remains noteworthy (Fig. 6C & D).

Microglia branch points and branch lengths provide insights into the relative differences in ramification and process complexity. Branch points were classified as primary if a filament intersected the soma, with the branch counted as primary until a branch not originating from the soma intersected it (Fig. 6A). Secondary branch points were identified as locations along primary branches where the intersection occurred (Fig. 6A). Secondary branching included all subsequent branches not deemed primary (Fig. 6A). Using these classifications, we found no effect of time of day on the number of primary and secondary branch points (Two-way ANOVA: primary branch points, $F_{1,11}$ =1.743, $p = 0.214$; secondary branch points, $F_{1,11} = 0.015$, $p = 0.905$) (Fig. 6E & F). We

also did not observe an effect of sex on primary or secondary branch points (Two-way ANOVA: primary branch points, $F_{1,11} = 0.225$, $p = 0.624$; secondary branch points, $F_{1,11} = 0.398$, $p = 0.905$), or an interaction (Two-way ANOVA: primary branch points, F $F_{1,11} = 0.069$, $p = 0.798$; secondary branch points, $F_{1,11} = 1.828$, p = 0.204). This may reflect a lack of difference in process complexity between times of day and sexes. There was also no observed difference in the length of primary branches between the two times of day (Two-way ANOVA, $F_{1,11}= 0.244$, $p = 0.631$) or sexes (Two-way ANOVA, $F_{1,11}= 0.554$, $p = 0.472$), and there was no interaction effect (Two-way ANOVA, $F_{1,11}= 1.205$, $p = 0.296$) (Fig. 6G). This further demonstrates a lack of difference in ramification and process complexity between times of day and sexes.

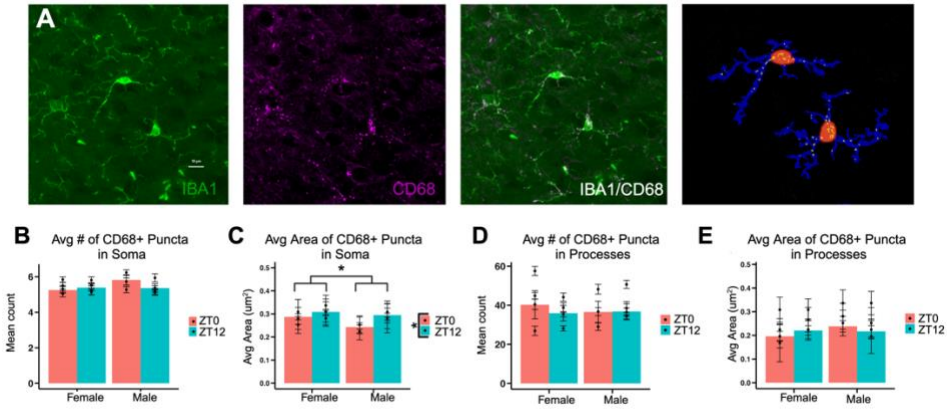

Figure 7. Time-of-day influences CD68+ puncta in the soma of microglia in the PFC. (A) Representative image demonstrating colocalization of IBA1, DAPI, and CD68 in order to identify CD68+ puncta in the cell body (yellow colocalized with orange) and in the processes (yellow colocalized with blue). (B) Average number of CD68+ puncta in individual somas (C) Average area of CD68+ puncta localized in the soma. (D) Average number of CD68+ puncta in microglia processes. (E) Average area of CD68+ puncta localized in microglia processes. n = 3-4 mice per group. B and D data show mean ± SEM, C and E data show mean of median +SEM , *p < 0.05. Magnification bar = 10 µm.

The ability of microglia to perform phagocytosis distinguishes them from many other cells in the CNS (Kono et al., 2021). CD68 is localized to microglial phagosomes and is often used as a proxy to measure phagocytic activity (Boche et al., 2012). We

measured the number and area of CD68+ puncta colocalized with IBA1+ cells (Fig. 7A). A raw count and area of each CD68+ puncta were calculated from an average of 124,000 CD68+ puncta per group (31,000 CD68+ puncta per animal). The count and area of CD68+ puncta were further distinguished by localization to either the soma or processes (Fig. 7A). These distinctions reflect different morphological and functional states of microglia. For example, phagocytic activity occurring in the processes may be indicative of the ball-and-chain microglia morphology, a state in which microglia phagocytose smaller bits of material, such as synapses (Vidal-Itriago et al., 2022).

Our analysis revealed no significant main effect of ZT (Two-way ANOVA, $F_{1,11} = 0.383$, $p = 0.549$), or of sex (Two-way ANOVA, $F_{1,11} = 1.155$, $p = 0.306$), on the number of CD68+ puncta. Additionally, there was no significant interaction between ZT and sex (Two-way ANOVA, $F_{1,11} = 1.734$, $p = 0.215$). These results indicate that in the soma, there was no observed difference in the average number of CD68+ puncta per microglia cell across the conditions (Fig. 7B). However, we did find a main effect of ZT on the average area of CD68+ puncta in the soma (Two-way ANOVA, $F_{1,11} = 9.49$, $p = 0.0091$) and a main effect of sex (Two-way ANOVA, $F_{1,11}= 5.308$, $p = 0.0417$), but no interaction effect (Two-way ANOVA, $F_{1,11}= 1.857$, $p = 0.200$) (Fig. 7C). Specifically, there was a significant increase in the average area of CD68+ puncta in the soma at ZT12 compared to ZT0 (Fig. 7C). With regards to the number of and area of CD68+ puncta in the processes, we did not discover a difference between the two time points (Two-way ANOVA: count, $F_{1,11} =0.169$, $p = 0.689$; area, $F_{1,11} = 0.025$, $p = 0.878$) (Fig. 7D & E). We also did not observe an effect of sex on the count or area of CD68+ puncta in the processes (Two-way ANOVA: count, $F_{1,11} = 0.064$, $p = 0.805$; area, $F_{1,11} = 0.636$, $p =$

0.442), or an interaction (Two-way ANOVA: count, F $F_{1,11}$ = 0.181, p = 0.678; area, $F_{1,11}$ = 1.034, p = 0.331) (Fig. 7D & E). Newly formed lysosomes, tend to be smaller; as they mature, accumulate more substrates, and fuse with phagosomes and late endosomes, they grow in size (Yang & Wang, 2021). The size of lysosomes is also directly related to the size of digested material (Cooper, 2000). The larger area of CD68+ puncta at ZT12 may reflect more mature lysosomes filled with accumulated material. This suggests more active degradation processes at ZT12.

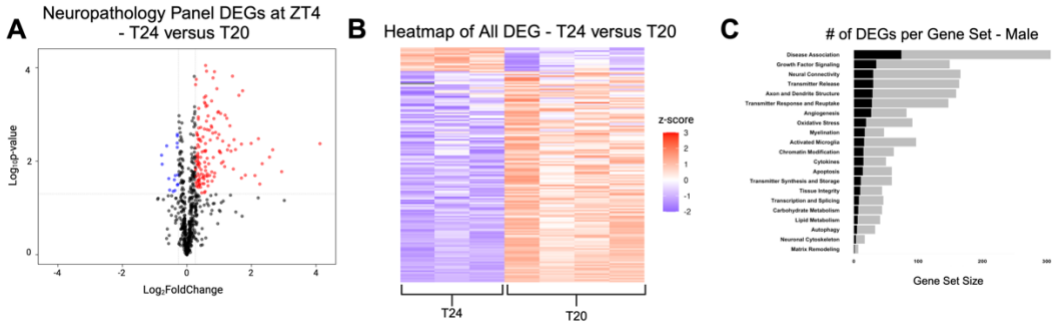

Figure 8. Effect of T20 circadian desynchronization on the expression of neuropathology-related genes. (A) Volcano plot depicting differential gene expression from the nCounter Mouse Neuropathology Panel under T20 conditions when compared to T24 controls (159 differentially expressed/760 total genes, 21%). (B) Heatmap displaying all significantly differentially expressed genes across conditions in the nCounter Mouse Neuropathology Panel in male mice. (C) Bar graph showing the number of genes associated with each nCounter Mouse Neuropathology Panel Gene Set and the number of differentially expressed genes within each annotation in male mice. The total number of genes per annotation is represented by the full bar height, while the shaded portion indicates the subset of differentially expressed genes. n = 3-4 mice per group. Significance reported when p < 0.05 and Fold Change > Log2|1.2|.

As there seems to be an effect of time-of-day on PFC tissue and characteristics of resident microglia, we were interested in uncovering the effect of circadian desynchronization on these same characteristics. To address the effect of perturbations of circadian rhythm on gene expression in the prefrontal cortex of mice, animals were subject to either a normal 12hr light: 12hr dark (T24) condition, or a 10hr light: 10hr dark

(T20) circadian desynchronization condition. PFC tissue from control and ECD male mice was collected at ZT4 and then analyzed using Nanostring transcriptomics on the nCounter Mouse Neuropathology Panel as previously described. Of the 760 transcript probes included in this panel, we observed 159 (21%) differentially expressed mRNA transcripts under T20 conditions when compared to T24 controls (Fig. 8A). The majority of the neuropathology-related DEGs are upregulated under T20 conditions (143/159, 90%) (Fig. 8B) and fall under a variety of biological pathway associations (Fig. 8C). These results indicate an exacerbation of neuropathological processes under the T20 condition. The five gene sets with the greatest number of DEGs are "Disease Association," "Growth Factor Signaling," "Neuronal Connectivity," "Transmitter Release," and "Axon and Dendrite Structure" (Fig. 8C). An upregulation of genes in these pathways suggests altered neuronal function and response to pathology in animals under T20 lighting conditions. Intriguingly, all these pathways involve microglia function.

When examining the "Activated Microglia" gene set, a total of 16 genes were found to be upregulated under T20 treatment (Fig. 9A). This upregulation of genes may reveal an increase in microglia activation due to the T20 ECD model, a phenomenon seen under other circadian disruption models, such as chronic jet lag (Meng et al., 2023). In accordance with an increase in microglia activation, we observed a significant increase in the normalized expression of *Cd68* (simplified negative binomial model, $p = 0.017$) (Fig. 9B). This finding suggests that microglia are more likely to be found in an "active" state or engaged in phagocytosis under the experimental conditions (T20).

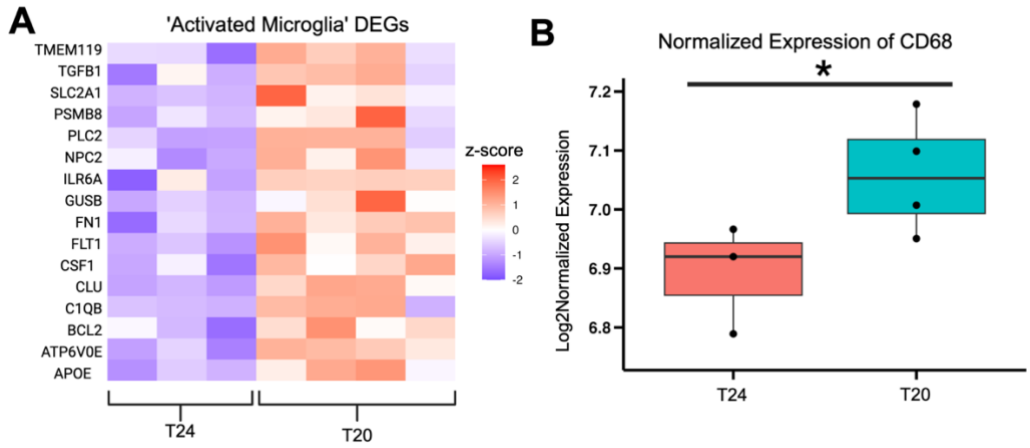

Figure 9. A model of T20 circadian desynchronization induces upregulation in the expression of "microglia-related" transcripts in the prefrontal cortex of male mice**.** (A) Heatmap of significantly differentially expressed genes between T24 control and T20 in the 'Activated Microglia' Gene Set in male mice. (B) Normalized expression of CD68 under T24 and T20 conditions. n=3-4 mice per group. *p < 0.05.

The next step was to assess the morphological and phagocytic characteristics of microglia in the prefrontal cortex as previously described. Animals from the T20 and control groups were collected at the onset of the dark phase, with T24 and T20 animals collected at ZT12. We employed the same detection recipe and defined characteristics as described in the TOD experiment. We discovered a main effect of T20 treatment on the number of IBA1+ cells in the prefrontal cortex (PFC) (Two-way ANOVA: $F_{1,20} = 9.846$, $p = 0.005$), but did not observe a main effect of sex (Two-way ANOVA: $F_{1,20} = 0.454$, $p = 0.508$) or an interaction effect (Two-way ANOVA: $F_{1,20} = 0.036$, $p = 0.852$) This suggests that there was a marked decrease in the number of IBA1+ cells under T20 conditions.

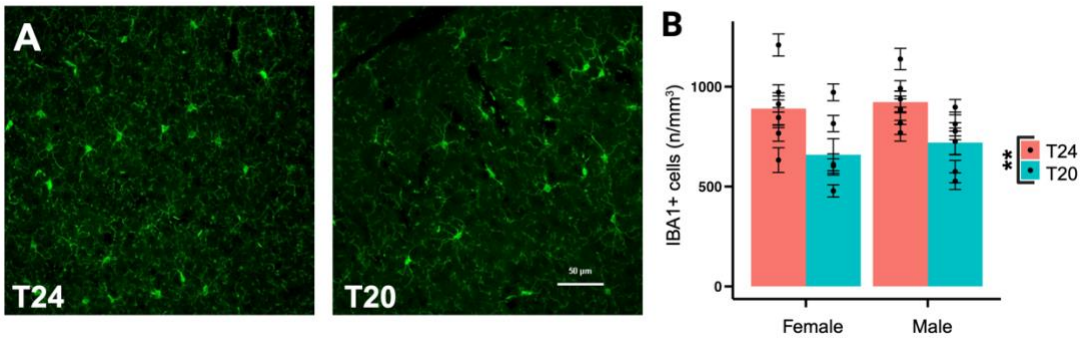

Figure 10. Circadian desynchronization decreases the number of IBA1+ cells in the PFC of male and female mice. (A) Representative 40x images from male mice under T24 control and T20 conditions. (B) Quantification of IBA1+ cell counts in male and female mice under T24 control and T20 conditions. n= 6 mice per group. All data show mean ± SEM, *p < 0.05. Magnification bar = 50 µm.

Although we did not observe a main effect of the T20 treatment on average soma size (Two-way ANOVA: $F_{1,20} = 1.876$, $p = 0.186$) or sex (Two-way ANOVA: $F_{1,20} = 0.377$, $p = 0.186$), nor an interaction effect (Two-way ANOVA: $F_{1,20} = 0.401$, $p = 0.534$), we noted a skewed distribution in soma size (Supplemental Fig. 2), similar to the distribution observed in the time-of-day characterization. Consequently, we applied a similar binning approach to categorize soma sizes and completed a chi-squared test of independence. The results revealed a significant effect of ZT on the distribution of soma size bins in female mice ($\chi^2(2) = 59.306$, $p < 0.0001$). A similar difference was observed in males ($\chi^2(2) = 17.006$, $p = 0.0002$). The soma size bins were analyzed by sex and we discovered no significant interaction between soma size groupings and treatment in males (t-test: 20-40; t= -0.124, $p = 0.9037$, 40-80; t= -0.3264, p=0.751, 80-120; t=-1.332, p= 0.213 or in females (t-test: 20-40; t= 1.068, $p = 0.3124$, 40-80; t= -0.949, *p=0.367*, 80-120; t=1.119, p= 0.289). The presence of distinct distribution patterns suggests potential underlying mechanisms that warrant further investigation.

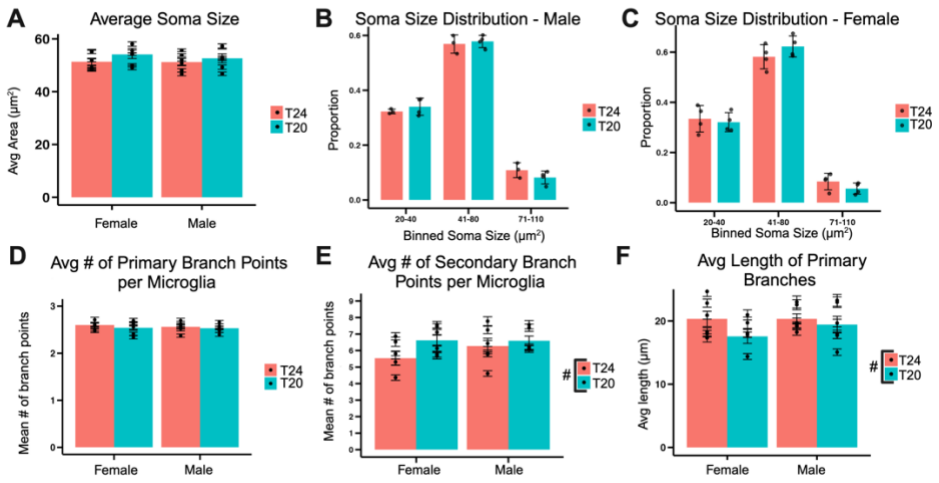

Figure 11. Effects of circadian desynchronization on morphological characteristics of IBA1+ cells in the PFC of male and female mice. (A) Average soma size of microglia cells under T24 and T20 conditions in male and female mice. (B) Proportions of microglia soma sizes within size bins by treatment in male and (C) female mice. (D) Average number of primary branch points per microglia cell soma in males and females between T24 and T20 conditions. (E) Average number of secondary branch points per microglia cell soma in males and females T24 and T20 conditions (F) Average length of primary branch points in males and females T24 and T20 conditions. n = 6 mice per group. All data show mean ± SEM, # $p < 0.1$, * $p < 0.05$.

Following this, we analyzed the relative differences in ramification and process complexity between the groups. We did not observe a significant main effect of treatment on the number of primary branch points (Two-way ANOVA: $F_{1,20} = 0.308$, $p = 0.585$) or a main effect of sex (Two-way ANOVA: $F_{1,20} = 0.891$, $p = 0.356$). We also did not observe an interaction effect (Two-way ANOVA: $F_{1,20} = 0.129$, $p = 0.723$).

However, we observed a trend towards a main effect of treatment on the number of secondary branch points (Two-way ANOVA: $F_{1,20} = 3.23$, $p = 0.08$). We did not see a main effect of sex (Two-way ANOVA: $F_{1,20} = 0.851$, $p = 0.367$) or an interaction effect (Two-way ANOVA: $F_{1,20} = 0.957$, $p = 0.340$). This suggests that while the treatment does not significantly affect primary branch points, there may be a potential effect on

secondary branch points. Interestingly, there seems to be an increase in the number of secondary branch points under the T20 condition compared to the T24 control.

We also observed a trend towards a main effect of treatment on the length of primary branch points (Two-way ANOVA: $F_{1,20} = 3.86$, $p = 0.06$), with a reduction in primary branch length under T20 conditions. However, there was no significant main effect of sex (Two-way ANOVA: $F_{1,20} = 1.727$, $p = 0.204$) or interaction effect (Two-way ANOVA: $F_{1,20} = 0.768$, $p = 0.391$). Together, the change in number of branches and the trend in decreased branch length suggests that the T20 model influences changes in cell structure at the onset of the dark phase, perhaps to a more "activated", amoeboid.

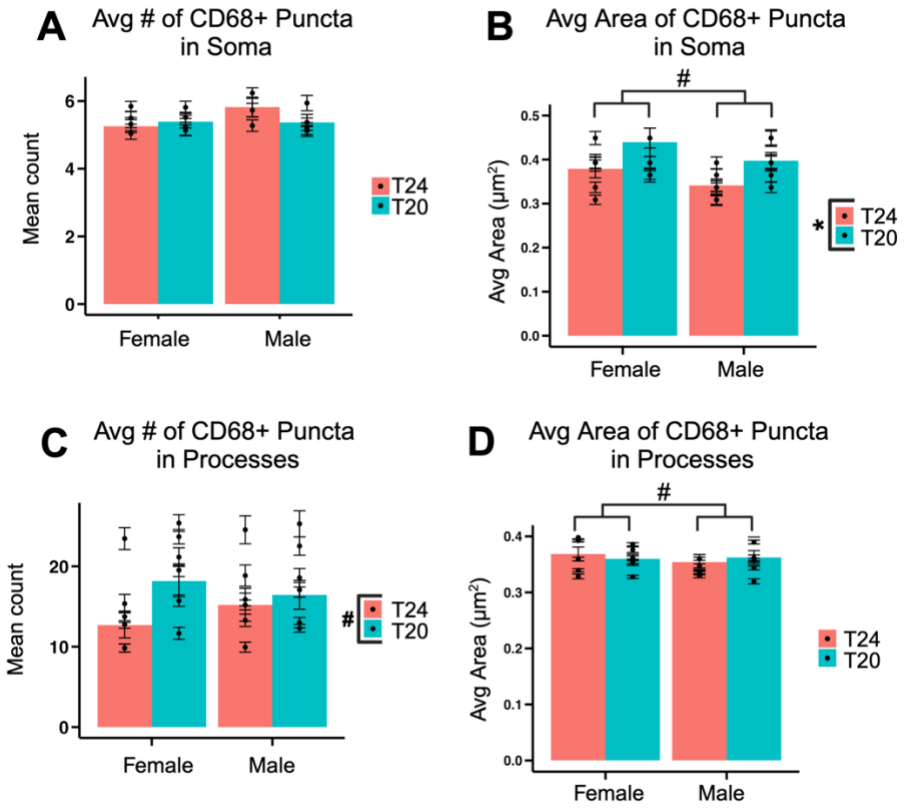

Figure 12. T20 circadian desynchronization induces changes in CD68+ puncta in the PFC. (A) Average number of CD68+ puncta in individual somas. (B) Average area of CD68+ puncta localized in the soma. (C) Average number of CD68+ puncta in microglia processes #. (D) Average area of CD68+ puncta localized in microglia processes . n = 6 mice per group. B and D data show mean ± SEM, C and E data show mean of median + SEM, # $p < 0.1$, * $p < 0.05$.

In assessing phagocytic characteristics of microglia between the two conditions, we found no main effect of treatment (Two-way ANOVA: $F_{1,20} = 0.042$, $p = 0.839$ or sex (Two-way ANOVA: $F_{1,20} = 2.899$, $p = 0.104$) on the number of CD68+ puncta in the soma. We also did not observe an interaction effect (Two-way ANOVA: $F_{1,20} = 1.265$, $p = 0.274$). However, we did find a main effect of treatment on the average area of CD68+ puncta in the soma (Two-way ANOVA: $F_{1,20} = 6.991$, $p = 0.0156$) and a trend in sex (Two-way ANOVA: $F_{1,20} = 3.233$, $p = 0.0873$), but no interaction effect (Two-way ANOVA: $F_{1,20} = 0.001$, $p = 0.917$). An increased size of CD68+ puncta in the soma may reflect the uptake of larger cargo or enhanced phagocytic activity, suggesting more activated microglia under T20 conditions.

We also observed a trend towards a main effect of treatment on the number of CD68+ puncta in the processes ($F_{1,20} = 3.639$, $p = 0.086$), but no main effect of sex ($F_{1,20} = 0.048$, $p = 0.829$) or interaction effect ($F_{1,20} = 1.305$, $p = 0.267$). We also observed a trend towards a main effect of sex on the average area of CD68+ puncta in the processes (Two-way ANOVA: $F_{1,20} = 3.049$, $p = 0.0961$, but no main effect of treatment (Two-way ANOVA: $F_{1,20} = 0.122$, $p = 0.7306$) or interaction effect (Two-way ANOVA: $F_{1,20} = 0.122$, $p = 0.7306$). An increase in the number of CD68+ puncta may represent overall increased phagocytic activity by microglial cells, particularly in their processes. Phagocytic activity in the processes often indicates the uptake of smaller material, such as synapses and cellular debris (Vidal-Itriago et al., 2022).

Overall, our results on microglia morphology and phagocytic potential suggests that a model of T20 circadian disruption induces alterations in microglial function and

structure, potentially affecting their role in neuroinflammation and brain homeostasis during the dark phase of the circadian cycle.

2.4 Discussion

We aimed to investigate the role of biological time and perturbations of circadian rhythm on the morphology and function of microglia in the prefrontal cortex of male and female mice. This investigation was carried out using a dual approach: gene expression analysis and immunohistochemistry combined with imaging.

Under physiological conditions, we found significant differences in the expression of several mRNA transcripts in the PFC of mice at ZT16 versus ZT4. A greater number of genes in this panel were differentially expressed across time of day in male mice compared to female mice. Of the mRNA transcripts differentially expressed in both sexes, all genes showed the same direction of expression, alluding to a consistent regulatory mechanism that is independent of sex. These DEGs belonged to a wide range of functional pathways, including “Disease Association,” “Growth Factor Signaling,” and “Axon and Dendrite Structure” in both sexes, indicating a time-of-day effect on these pathways in the PFC. Previous studies have shown sex-specific differences in the expression of a limited set of genes (e.g., GluA1 and GluA2) in the PFC (Knouse et al., 2022), often under chronic stress conditions (Brivio et al., 2020). These transcriptional variations suggest differential responses to external challenges between sexes, potentially leading to distinct health outcomes.

Many of the pathways containing DEGs are mediated by microglial activity. In males, there was more upregulation of genes in the “Activated Microglia” gene set at ZT16 compared to ZT4. This suggests a potential time-of-day effect on microglial

function, with an increase in activity at ZT16. Upregulation of genes such as *Il6ra,* and *Il1r1* has been linked to an increase in proinflammatory microglia cells (Burton et al., 2013; Basu et al., 2004). Previous work has shown that male microglia demonstrate increased pro-inflammatory activation (Guneykaya et al., 2018), a finding we have recapitulated in the PFC. In female mice, only three microglia-related genes—P2XR4, XBP1, and FN1—exhibited time-of-day variations. These genes also demonstrated differential expression in males, indicating a fundamental role for the specific timing of their regulation in microglial function. The limited number of differentially expressed microglia-related genes in females makes it challenging to interpret the implications of these changes.

Under T20 conditions, we found a large number of differentially expressed genes, with a majority of these being upregulated with respect to control conditions. The large number of DEGs suggests the T20 model induces an increase in neuropathological processes at ZT4 in male mice. Specific pathways of interest included "Axon and Dendrite Structure" and "Neuronal Connectivity" as previous work has demonstrated that this model induces changes in dendrite arborization and electrophysiological properties in the PFC (Karatsoreos et al., 2011; Roberts & Karatsoreos, 2023).

We also discovered an upregulation of genes belonging to the 'Activated Microglia' gene set under T20 conditions. These genes include transmembrane protein 119 (*Tmem119*), a highly specific marker for microglia (Ruan & Elyaman, 2022), and *Il6ra,* a receptor involved in activation of microglia (Burton et al., 2013). The summation of upregulation of these genes suggests the T20 model may increase microglia activation and phagocytic capacity under the T20 condition, at least during the light phase, in male

mice in the PFC. Our findings are similar to previous work in the hippocampus, which demonstrated an increase in microglial activation and phagocytic capacity (protein expression of CD68) following chronic jet lag (Meng et al., 2023).

To elucidate the downstream effects of differential mRNA transcript expression, we performed triple-label immunohistochemistry staining and imaging using the automated TissueFaxSL cytometry microscope, which allowed us to capture extensive regions of interest. To complete image analysis, we developed a novel, unbiased detection method for the comprehensive characterization of microglia across large datasets. The detection method we developed effectively eliminates the bias associated with manual, researcher-generated skeletons. It is also time-efficient and easier to use than machine learning techniques, as it does not have to be retrained between staining sessions and image acquisition. Additionally, the method is customizable between runs and versatile for various cell types.

Under physiological conditions, we observed time-of-day variations in several morphological characteristics of microglia, including a novel increase in the number of microglial cells under physiological conditions at ZT0 versus ZT12. Under a T20 model of ECD, we observed a decrease in the number of IBA1+ cells in the PFC under T20 conditions compared to T24. This finding was unexpected and has not been previously observed in other brain areas (Meng et al., 2023). Changes in the number of microglial cells in a specific region of tissue has been shown to be correlated to proliferation of surrounding tissue under physiological states (Tay et al., 2017). Under an acute neurodegeneration model, proliferation occurs locally by clonal expansion of microglia cells (Tay et al., 2017). Other mechanisms by which microglial numbers may change in a

specific region include apoptosis (Askew et al., 2017) and migration to sites within tissue (Boghozian et al., 2023). Further investigation into the mechanism by which time-of-day and ECD affect the number of microglia cells and the functional impact of this change is required.

Interestingly, we discovered a distinct distribution of soma sizes across ZTs, treatments, and sexes. This hints towards biologically relevant soma size differences that remain consistent across different experimental conditions and time points in the PFC. The functional meaning of these distinct soma size groups is unknown and requires further research.

We did not observe a time-of-day effect in process complexity and ramification, suggesting that time-of-day does not impact the overall morphological complexity of microglial cells. Previous work has demonstrated a time-of-day influence on the complexity of microglia in the somatosensory cortex of male mice (Hayashi et al., 2013). Microglia are heterogeneous between brain regions (Grabert et al., 2016), and it is possible that PFC microglia are phenotypically different from other brain region microglia. In other words, time of day may not influence PFC microglia in the same way as microglia from other brain regions, such as the somatosensory cortex (Hayashi et al., 2013).

Although we did not observe an effect of time-of-day, we discovered a trend towards a decrease in primary branch length in mice under T20 conditions, indicative of retracted processes and a more “activated” microglial state (Vidal-Itriago et al., 2022). This observation has also been reported in the hippocampus of mice subjected to chronic circadian desynchronization (Meng et al., 2023). Interestingly, we see a trend towards an

increase in the number of secondary branch points. This observation is often indicative of hyper-ramified microglia, cells characterized by an extensive and highly branched morphology (Vidal-Itriago et al., 2022). Hyper-ramified microglia are typically associated with increased synaptic remodeling and potentially enhanced surveillance of the neuronal environment morphology (Vidal-Itriago et al., 2022). The increased branching could reflect an adaptive response to alterations in brain tissue, potentially related to the observed changes in phagocytic activity and synaptic pruning. Microglia are morphologically heterogeneous within brain regions, as changes in activity are dependent changes in the local microenvironment (Smolders et al., 2019), and thus under T20 conditions may display a range of morphological phenotypes.

In relation to phagocytic activity, we observed an increase in the area of CD68+ puncta in the soma at ZT0 compared to ZT12. Larger CD68+ puncta could indicate either the size of the material being engulfed (Cooper, 2000) or the stage of degradation (Yang & Wang, 2021). A similar finding of increased CD68+ microglia in the hippocampus of rats at ZT0 has been reported (Choudhury et al., 2020). Under T20 conditions, we also observed an increase in the area of CD68+ puncta in the soma and a trend towards an increase in the number of CD68+ puncta in the processes. The trend towards more CD68+ puncta in the processes might indicate increased phagocytic activity at the synaptic level, reflecting heightened synaptic pruning or removal of synaptic material. This pattern could suggest that T20 conditions influence both the overall phagocytic capacity and the specific activity related to synaptic pruning. We also saw a trend towards an effect of sex on the size of CD68+ puncta in the processes. Previous work has

shown sex-differences in the phagocytic activity of postnatal microglia (Yanguas-Casás et al., 2018).

The summation of changes to microglia morphology and phagocytic capacity suggests that a model of T20 circadian disruption not only influences characteristics mediated by time-of-day effects, but induces broader alterations in microglial function and structure, potentially affecting their role in neuroinflammation and brain homeostasis during the dark phase of the circadian cycle. These effects do not seem to be sex-specific in the PFC.

Our transcriptomics approach provides valuable insights into time-of-day differences in PFC tissue. However, it's important to note that our current gene analysis is not cell specific. To gain a more detailed understanding of how gene expression changes specifically impact microglia, we can employ single-cell RNA sequencing. We have tissue samples from both sexes at six different times of day (ZT0, ZT4, ZT8, ZT12, ZT16, ZT20), and the next logical step is to increase the number of animals per group to account for within-group variability and extend our analysis to additional time points. This will not only allow us to draw conclusions about other times of day but also assess the rhythmicity of gene expression patterns.

Additionally, we have tissue from male and female mice subjected to T20 conditions at various times of day, which we will compare to T24 time points to determine how the T20 model affects rhythmic gene expression. We aim to identify whether the observed activation represents a shift in the timing of rhythms or an overall disruption of circadian rhythms.

We also have the opportunity to refine and optimize our detection methods, incorporating additional characteristics. An exciting next step would be to conduct a phagocytosis assay coupled with live imaging, leveraging the capabilities of our microscope. This would enable us to establish a causal relationship between time-of-day and phagocytic activity.

Overall, we observed a significant time-of-day difference in the transcription of neuropathology-related genes between ZT4 and ZT16, with a notably larger difference in males. Specifically, there was an upregulation of activated microglia genes at ZT16 in males. We also detected a time-of-day variation in phagocytic capacity that was consistent across sexes, though other characteristics did not show notable fluctuations. Under T20 conditions, we found an overall upregulation of neuropathology-related genes, including increased expression of "activated microglia" mRNA transcripts. Additionally, T20 conditions affected microglia morphology and phagocytic capacity, resulting in a more activated microglial phenotype.

3. Supplemental Methods: IHC and Image Analysis Pipelines

While optimizing the immunohistochemistry (IHC) to imaging and analysis pipeline, several challenges arose. The first major challenge involved autofluorescence (AF) observed within microglia cells during confocal microscopy imaging. Previous research has shown that autofluorescent puncta localized within microglia can be easily mistaken for engulfed material within phagosomes (Stillman et al., 2023). In this study, distinguishing AF signals from CD68+ puncta proved difficult, complicating the assessment of microglial phagocytic activity.

To address this challenge, we developed a cost-effective, self-constructed photobleacher to quench AF in brain tissue before staining. The photobleacher was built using a combination of previously described protocols (Stillman et al., 2023; Sun et al., 2017). Given our lab's prior observations of significant AF in olfactory bulb (OB) tissue, we conducted testing on OB samples. We compared control slides incubated in phosphate buffer (PB) for 48 hours at 4°C with slides treated in the same manner but within our photobleaching unit. Our antibodies fluoresce under FITC (IBA1), DAPI, and CY5 (CD68), but not CY3. After performing identical IHC staining, we analyzed AF in the CY3 channel. The comparison revealed that photobleaching significantly reduced AF in OB tissue without affecting the fluorescence of our target stains, confirming that fluorescence in the CY5 channel originated from CD68 and was not confounded by AF (Supplemental Fig. 3).

A second challenge was to image a large area of the brain at a high enough resolution and with sufficient tissue depth to assess potential morphological changes within microglia. In other papers, while microglial morphology was assessed, these

measures were made in a handful of random parts of a brain area, and with a rather small number of microglia. Manual and semi-manual approaches typically assess between 10-500 microglia cells per animal (Reddaway et al., 2023). To overcome this challenge, and provide a far more comprehensive assessment, we utilized the fully automated TissueFaxSL cytometry microscope to capture large regions of interest with minimal human intervention. Opting for an automated spinning disk confocal microscope over a laser scanning microscope provided several advantages, including increased data collection speed and a hands-off approach after the initial setup. Driven by our interest in capturing Z-stacks to fully visualize the complex nature of microglia cells, we pioneered the use of the TissueFaxSL for 3D image collection, necessitating the development of a new image analysis pipeline.

The TissueFaxSL cytometry microscope typically uses the TissueFAXS software suite developed by TissueGnostics. However, due to limited experience with this software among UMass Light Microscopy Facilities staff, we opted to perform image analysis using NIS Elements, a commonly used image processing software. NIS Elements was unable to handle the volume of data generated by the TissueFaxSL microscope, leading to some tissue being unusable for analysis; 20-micron Z-stacks were reduced to 10-microns.

To address this challenge, we needed to design a new image analysis pipeline. Prior to image analysis in NIS Elements, we had to convert images from TissueGnostics into a compatible file type through a multi-step conversion process. After extensive troubleshooting, we optimized a pathway for conversion and analysis. Images were exported from TissueGnostics and converted to a format readable by NIS Elements in

ImageJ using a personalized macro (Fiji). TIFF files were then modified to set up proper channel properties for post-imaging analysis. The macro we developed ensures that the TIFF images are correctly interpreted and visualized according to their specific fluorescence properties during subsequent analysis (NIS Elements, v.6).

After optimizing this pipeline, we tackled the challenge of creating an appropriate detection method applicable across many images. After months of trial and error, we developed a GA3 recipe (NIS Elements, v.6) capable of quantifying a range of microglial characteristics across a large dataset. A simplified explanation of the GA3 recipe is as follows (Supplemental Fig. 4): During pre-processing, a maximum intensity projection was applied along with background reduction to enhance image quality. Soma identification was achieved through the colocalization of IBA1 and DAPI, with filtering based on area, shape, and fluorescence intensity. For filament identification, a threshold was set to identify filament structures within a specific area around the soma. Segmentation involved using the medial axis and soma outline to create a rough skeleton, followed by filling any holes to correct discrepancies in fluorescence. A watershed algorithm was applied from the soma to differentiate between branches of different cells. Branch points were categorized into primary and secondary based on localization to the soma. Secondary branches were defined as those with both an endpoint and a secondary branch point, whereas primary branches extended from the soma and included all branches not classified as secondary.

We applied out recipe using the batch analysis feature. This function allows for the processing of large datasets with no user input, saving considerable time for researchers. Using this detection method, we were able to automatically quantify

microglial characteristics within approximately 100 cubic micrometers of tissue per animal, with each animal's analysis taking about an hour.

As far as we know, we are the first group to use a GA3 recipe in NIS Elements for batch analysis of microglia-related characteristics. The automated approach enhances consistency across tissues and groups. A significant advantage of NIS Elements is that it does not require coding expertise. The GA3 recipe we developed is modular and can be easily adapted to fit different tissue regions and imaging sessions without the need for retraining periods, unlike machine learning analyses. This GA3 recipe has the potential to be applied to different brain regions and cell types, thanks to the ease of adjusting thresholds.

While our approach has helped us to overcome several key challenges, there are technical limitations in our solution. The characterization of microglia is only as good as the detection method created. Inter-user reliability may be compromised if users individualize the detection recipe with unique thresholds. Additionally, the effectiveness of the GA3 recipe is dependent on the quality of the staining and imaging. Specific problems we encountered included varying levels of fluorescence within tissue, potentially due to missing steps in the Z-stack or tissue integrity, which made it difficult for the program to detect certain filaments. Furthermore, when many branches were localized to one area of tissue, the GA3 recipe struggled to identify the soma associated with each branch. With the specific parameters set in our GA3, we were only able to address primary and secondary branches. This limitation can be addressed by creating a more detailed definition of branching levels within the GA3, which we will tackle soon. Additionally, while we are drawing conclusions about CD68+ puncta, the resolution of

this microscope may be too low to capture the full range of differences we want to observe. Solutions to these problems include higher magnification imaging, analysis on the 3D reconstruction of tissue, and further manipulation of our detection recipe.

This detection method is completely customizable, with comments included in the recipe to allow users to easily update it. With more time and a better handle on image output, this detection method has the potential to be influential across neuroscience and biological research.

4. Supplemental Figures

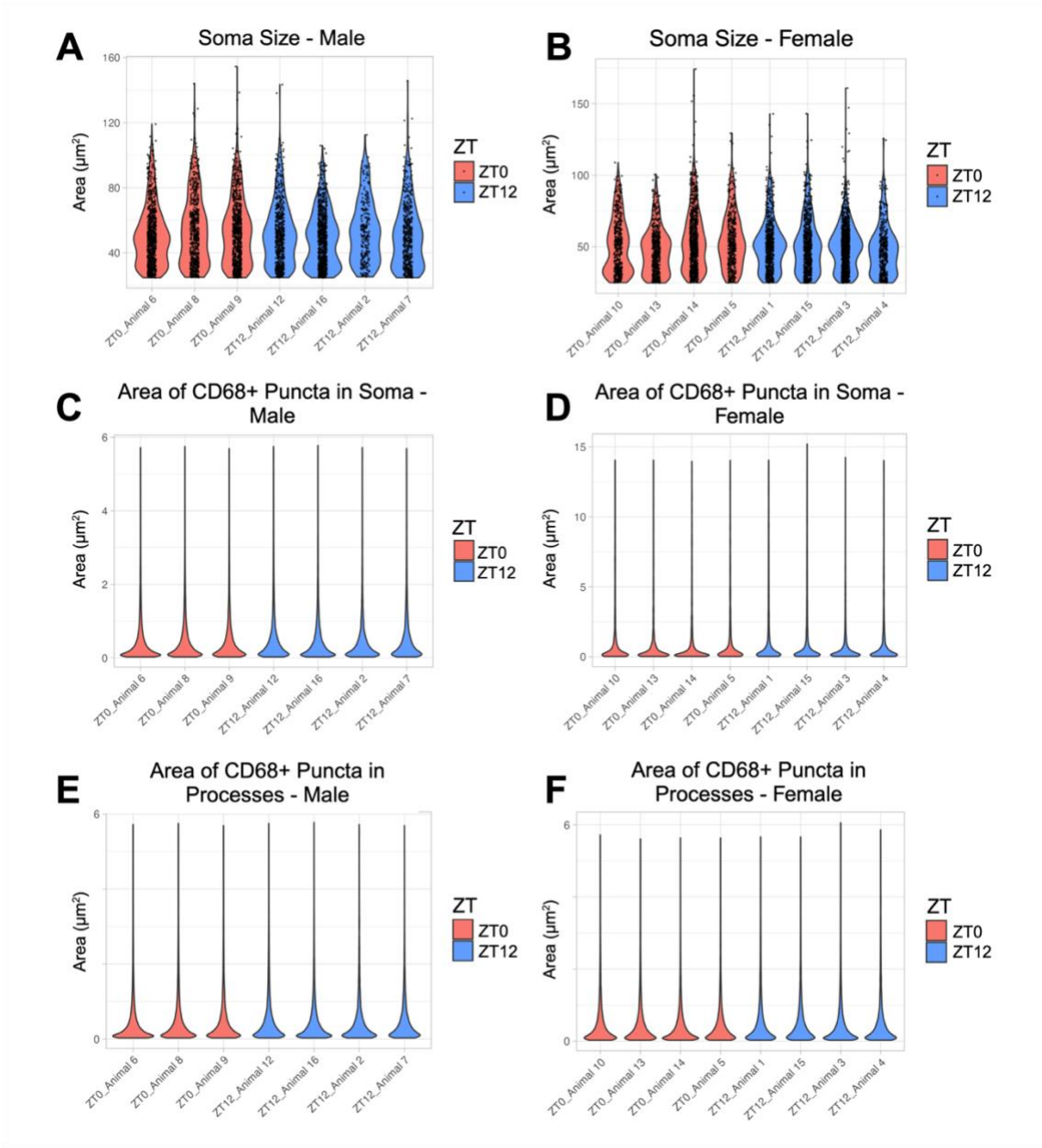

Supplemental Figure 1. Distribution of the area of soma sizes and CD68+ puncta in the soma and processes based on time-of-day in the PFC. (A) Violin plot depicting the distribution of microglia soma size in male and (B) female mice. Points represent the soma area of individual cells. (C) Violin plot depicting the distribution of CD68+ puncta area in the soma in male and (D) female mice. (E) Violin plot depicting the distribution of CD68+ puncta area in the processes of male and (F) female mice.

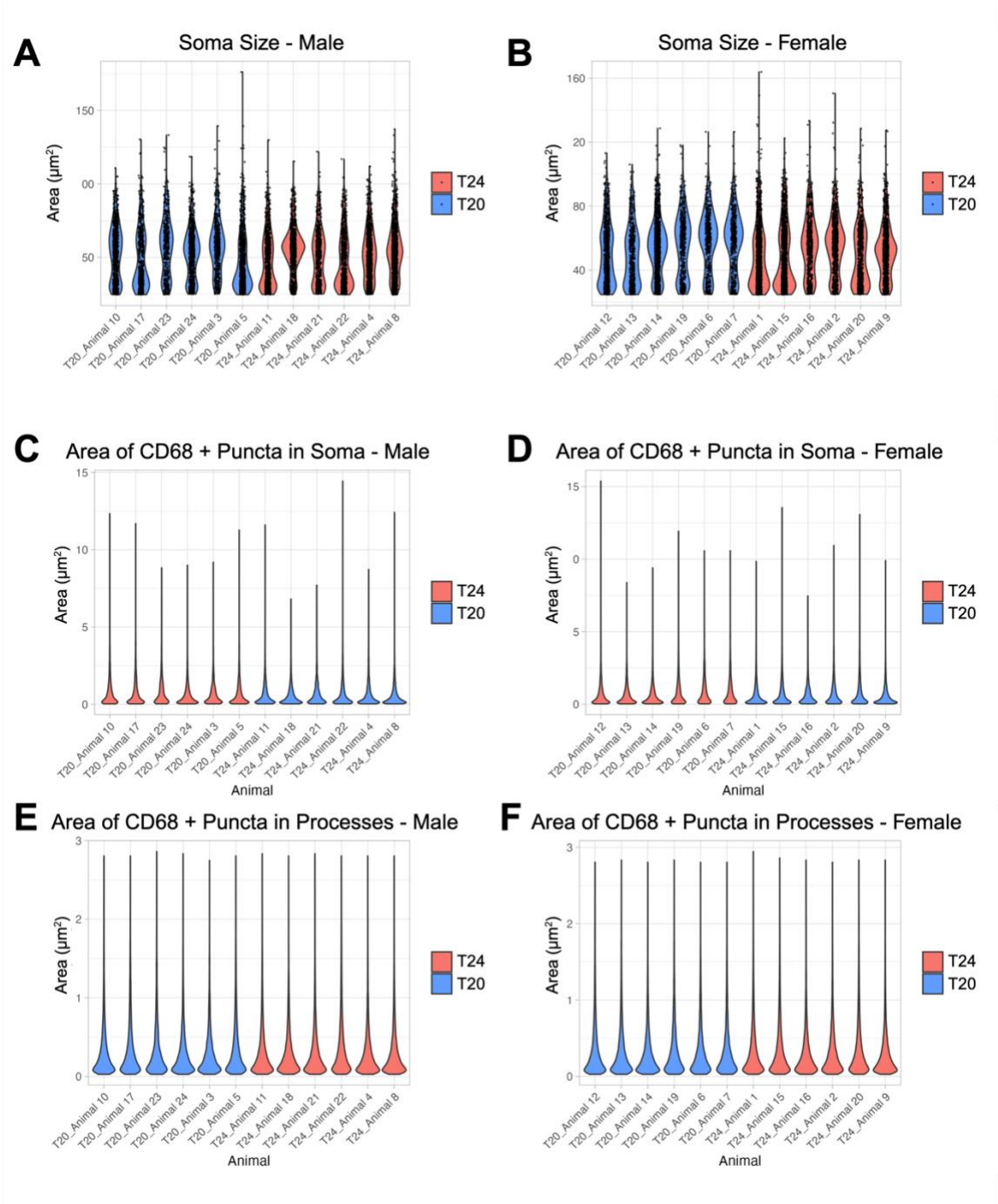

Supplemental Figure 2. Distribution of the area of soma sizes and CD68+ puncta in the soma and processes of mice under control and T20 conditions. (A) Violin plot depicting the distribution of microglia soma size in male and (B) female mice. Points represent the soma area of individual cells. (C) Violin plot depicting the distribution of CD68+ puncta area in the soma in male and (D) female mice. (E) Violin plot depicting the distribution of CD68+ puncta area in the processes of males and (F) female mice.

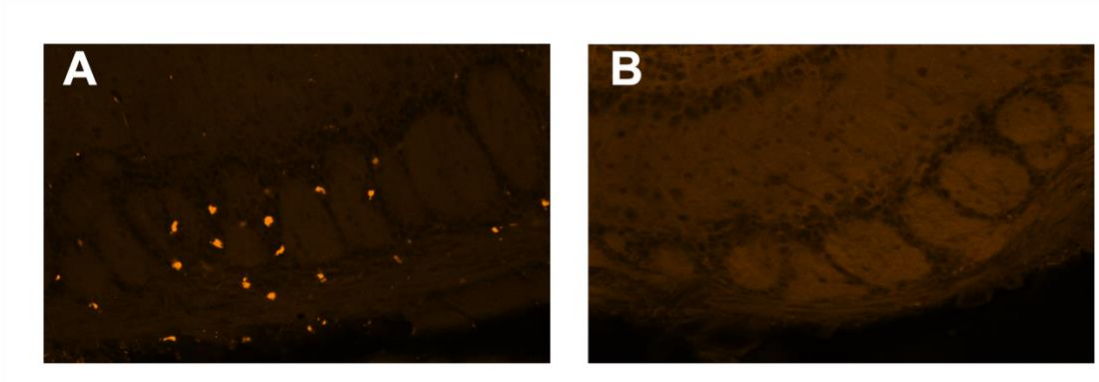

Supplemental Figure 3. Photobleaching steps to quench intrinsic autofluorescence in tissue. (A) Olfactory bulb tissue following original staining protocol. No antibodies are labeled in this channel. (B) Olfactory bulb tissue prepared with photobleaching prior to following original staining protocol.

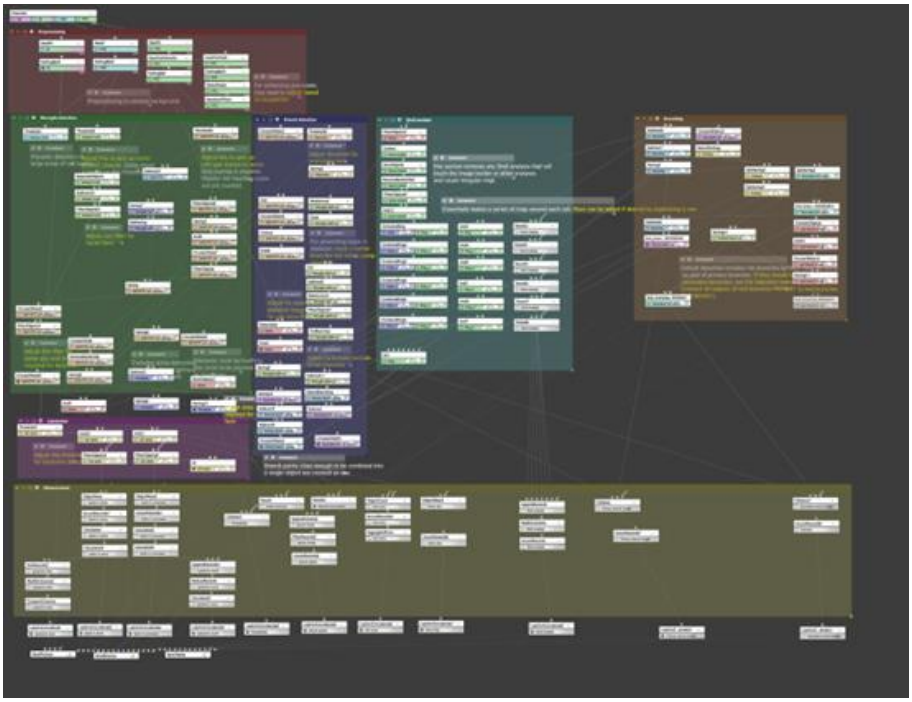

Supplemental Figure 4. GA3 recipe created for morphological assessment.

References

Abbott, S. M., Malkani, R. G., & Zee, P. C. (2020). Circadian disruption and human health: A bidirectional relationship. *European Journal of Neuroscience*, *51*(1), 567–583. https://doi.org/10.1111/ejn.14298

Abe, M., Herzog, E. D., Yamazaki, S., Straume, M., Tei, H., Sakaki, Y., Menaker, M., & Block, G. D. (2002). Circadian Rhythms in Isolated Brain Regions. *Journal of Neuroscience*, *22*(1), 350–356. https://doi.org/10.1523/JNEUROSCI.22-01-00350.2002

Antignano, I., Liu, Y., Offermann, N., & Capasso, M. (2023). Aging microglia. *Cellular and Molecular Life Sciences: CMLS*, *80*(5), 126. https://doi.org/10.1007/s00018-023-04775-y

Arble, D. M., Ramsey, K. M., Bass, J., & Turek, F. W. (2010). Circadian Disruption and Metabolic Disease: Findings from Animal Models. *Best Practice & Research. Clinical Endocrinology & Metabolism*, *24*(5), 785–800. https://doi.org/10.1016/j.beem.2010.08.003

Ashton, A., Foster, R. G., & Jagannath, A. (2022). Photic Entrainment of the Circadian System. *International Journal of Molecular Sciences*, *23*(2), 729. https://doi.org/10.3390/ijms23020729

Askew, K., Li, K., Olmos-Alonso, A., Garcia-Moreno, F., Liang, Y., Richardson, P., Tipton, T., Chapman, M. A., Riecken, K., Beccari, S., Sierra, A., Molnár, Z., Cragg, M. S., Garaschuk, O., Perry, V. H., & Gomez-Nicola, D. (2017). Coupled Proliferation and Apoptosis Maintain the Rapid Turnover of Microglia in the Adult Brain. *Cell Reports*, *18*(2), 391–405. https://doi.org/10.1016/j.celrep.2016.12.041

Baltazar, R. M., Coolen, L. M., & Webb, I. C. (2013). Diurnal rhythms in neural activation in the mesolimbic reward system: Critical role of the medial prefrontal cortex. *European Journal of Neuroscience*, *38*(2), 2319–2327. https://doi.org/10.1111/ejn.12224

Barnes, C. A., McNaughton, B. L., Goddard, G. V., Douglas, R. M., & Adamec, R. (1977). Circadian Rhythm of Synaptic Excitability in Rat And Monkey Central Nervous System. *Science*, *197*(4298), 91–92. https://doi.org/10.1126/science.194313

Basu, A., Krady, J. K., & Levison, S. W. (2004). Interleukin-1: A master regulator of neuroinflammation. *Journal of Neuroscience Research*, *78*(2), 151–156. https://doi.org/10.1002/jnr.20266

Boche, D., Perry, V. H., & Nicoll, J. a. R. (2013). Review: Activation patterns of microglia and their identification in the human brain. *Neuropathology and Applied Neurobiology*, *39*(1), 3–18. https://doi.org/10.1111/nan.12011

Boghozian, R., Sharma, S., Narayana, K., Cheema, M., & Brown, C. E. (n.d.). Sex and interferon gamma signaling regulate microglia migration in the adult mouse cortex in vivo. *Proceedings of the National Academy of Sciences of the United States of America*, *120*(29), e2302892120. https://doi.org/10.1073/pnas.2302892120

Borjigin, J., Zhang, L. S., & Calinescu, A.-A. (2012). Circadian Regulation of Pineal Gland Rhythmicity. *Molecular and Cellular Endocrinology*, *349*(1), 13–19. https://doi.org/10.1016/j.mce.2011.07.009

Brivio, E., Lopez, J. P., & Chen, A. (2020). Sex differences: Transcriptional signatures of stress exposure in male and female brains. *Genes, Brain and Behavior*, *19*(3), e12643. https://doi.org/10.1111/gbb.12643

Bunger, M. K., Wilsbacher, L. D., Moran, S. M., Clendenin, C., Radcliffe, L. A., Hogenesch, J. B., Simon, M. C., Takahashi, J. S., & Bradfield, C. A. (2000). *Mop3* Is an Essential Component of the Master Circadian Pacemaker in Mammals. *Cell*, *103*(7), 1009–1017. https://doi.org/10.1016/S0092-8674(00)00205-1

Burke, K. J., & Bender, K. J. (2019). Modulation of Ion Channels in the Axon: Mechanisms and Function. *Frontiers in Cellular Neuroscience*, *13*, 221. https://doi.org/10.3389/fncel.2019.00221

Burton, M. D., Rytych, J. L., Freund, G. G., & Johnson, R. W. (2013). Central inhibition of interleukin-6 *trans*-signaling during peripheral infection reduced neuroinflammation and sickness in aged mice. *Brain, Behavior, and Immunity*, *30*, 66–72. https://doi.org/10.1016/j.bbi.2013.01.002

Busche, M. A., & Konnerth, A. (2016). Impairments of neural circuit function in Alzheimer's disease. *Philosophical Transactions of the Royal Society B: Biological Sciences*, *371*(1700), 20150429. https://doi.org/10.1098/rstb.2015.0429

Chellappa, S. L., Morris, C. J., & Scheer, F. A. J. L. (2018). Daily circadian misalignment impairs human cognitive performance task-dependently. *Scientific Reports*, *8*, 3041. https://doi.org/10.1038/s41598-018-20707-4

Chistiakov, D. A., Killingsworth, M. C., Myasoedova, V. A., Orekhov, A. N., & Bobryshev, Y. V. (2017). CD68/macrosialin: Not just a histochemical marker. *Laboratory Investigation*, *97*(1), 4–13. https://doi.org/10.1038/labinvest.2016.116

Choudhury, M. E., Miyanishi, K., Takeda, H., Islam, A., Matsuoka, N., Kubo, M., Matsumoto, S., Kunieda, T., Nomoto, M., Yano, H., & Tanaka, J. (2020). Phagocytic elimination of synapses by microglia during sleep. *Glia*, *68*(1), 44–59. https://doi.org/10.1002/glia.23698

Christensen, R. N., Ha, B. K., Sun, F., Bresnahan, J. C., & Beattie, M. S. (2006). Kainate induces rapid redistribution of the actin cytoskeleton in ameboid microglia. *Journal of Neuroscience Research*, *84*(1), 170–181. https://doi.org/10.1002/jnr.20865

Citri, A., & Malenka, R. C. (2008). Synaptic Plasticity: Multiple Forms, Functions, and Mechanisms. *Neuropsychopharmacology*, *33*(1), 18–41. https://doi.org/10.1038/sj.npp.1301559

Cooper, G. M. (2000). Lysosomes. In *The Cell: A Molecular Approach. 2nd edition*. Sinauer Associates. https://www.ncbi.nlm.nih.gov/books/NBK9953/

Cornell, J., Salinas, S., Huang, H.-Y., & Zhou, M. (2021). Microglia regulation of synaptic plasticity and learning and memory. *Neural Regeneration Research*, *17*(4), 705–716. https://doi.org/10.4103/1673-5374.322423

Davidson, A. J., Sellix, M. T., Daniel, J., Yamazaki, S., Menaker, M., & Block, G. D. (2006). Chronic jet-lag increases mortality in aged mice. *Current Biology*, *16*(21), R914–R916. https://doi.org/10.1016/j.cub.2006.09.058

Dibner, C., Schibler, U., & Albrecht, U. (2010). The Mammalian Circadian Timing System: Organization and Coordination of Central and Peripheral Clocks. *Annual Review of Physiology*, *72*(Volume 72, 2010), 517–549. https://doi.org/10.1146/annurev-physiol-021909-135821

Doorn, K. J., Brevé, J. J. P., Drukarch, B., Boddeke, H. W., Huitinga, I., Lucassen, P. J., & van Dam, A.-M. (2015). Brain region-specific gene expression profiles in freshly isolated rat microglia. *Frontiers in Cellular Neuroscience*, *9*. https://doi.org/10.3389/fncel.2015.00084

Eyo, U. B., Peng, J., Swiatkowski, P., Mukherjee, A., Bispo, A., & Wu, L.-J. (2014). Neuronal Hyperactivity Recruits Microglial Processes via Neuronal NMDA Receptors and Microglial P2Y12 Receptors after Status Epilepticus. *Journal of Neuroscience*, *34*(32), 10528–10540. https://doi.org/10.1523/JNEUROSCI.0416-14.2014

Fairley, L. H., Lai, K. O., Wong, J. H., Chong, W. J., Vincent, A. S., D'Agostino, G., Wu, X., Naik, R. R., Jayaraman, A., Langley, S. R., Ruedl, C., & Barron, A. M. (2023). Mitochondrial control of microglial phagocytosis by the translocator protein and hexokinase 2 in Alzheimer's disease. *Proceedings of the National Academy of Sciences*, *120*(8), e2209177120. https://doi.org/10.1073/pnas.2209177120

Fishbein, A. B., Knutson, K. L., & Zee, P. C. (2021). Circadian disruption and human health. *The Journal of Clinical Investigation*, *131*(19). https://doi.org/10.1172/JCI148286

Fonken, L. K., Frank, M. G., Kitt, M. M., Barrientos, R. M., Watkins, L. R., & Maier, S. F. (2015). Microglia inflammatory responses are controlled by an intrinsic circadian clock. *Brain, Behavior, and Immunity*, *45*, 171–179. https://doi.org/10.1016/j.bbi.2014.11.009

Franco-Bocanegra, D. K., McAuley, C., Nicoll, J. A. R., & Boche, D. (2019). Molecular Mechanisms of Microglial Motility: Changes in Ageing and Alzheimer's Disease. *Cells*, *8*(6), 639. https://doi.org/10.3390/cells8060639

Gnocchi, D., & Bruscalupi, G. (2017). Circadian Rhythms and Hormonal Homeostasis: Pathophysiological Implications. *Biology*, *6*(1), Article 1. https://doi.org/10.3390/biology6010010

Grabert, K., Michoel, T., Karavolos, M. H., Clohisey, S., Baillie, J. K., Stevens, M. P., Freeman, T. C., Summers, K. M., & McColl, B. W. (2016). Microglial brain region−dependent diversity and selective regional sensitivities to aging. *Nature Neuroscience*, *19*(3), 504–516. https://doi.org/10.1038/nn.4222

Gu, X., Zhang, L., Zhao, Z., Fang, H., Zhao, T., Ju, S., Chen, X., Gao, W., Qian, X., Wang, X., Zhang, J., & Cheng, H. (2023). Imaging Microglia Surveillance during Sleep-wake Cycles in Freely Behaving Mice. *eLife*, *12*. https://doi.org/10.7554/eLife.86749

Guneykaya, D., Ivanov, A., Hernandez, D. P., Haage, V., Wojtas, B., Meyer, N., Maricos, M., Jordan, P., Buonfiglioli, A., Gielniewski, B., Ochocka, N., Cömert, C., Friedrich, C., Artiles, L. S., Kaminska, B., Mertins, P., Beule, D., Kettenmann, H., & Wolf, S. A. (2018). Transcriptional and Translational Differences of Microglia from Male and Female Brains. *Cell Reports*, *24*(10), 2773-2783.e6. https://doi.org/10.1016/j.celrep.2018.08.001

Gyoneva, S., & Traynelis, S. F. (2013). Norepinephrine Modulates the Motility of Resting and Activated Microglia via Different Adrenergic Receptors. *The Journal of Biological Chemistry*, *288*(21), 15291–15302. https://doi.org/10.1074/jbc.M113.458901

Harbison, C., Zhuang, K., Gettie, A., Blanchard, J., Knight, H., Didier, P., Cheng-Mayer, C., & Westmoreland, S. (2014). Giant cell encephalitis and microglial infection with mucosally transmitted simian-human immunodeficiency virus SHIVSF162P3N in rhesus macaques. *Journal of NeuroVirology*, *20*(1), 62–72. https://doi.org/10.1007/s13365-013-0229-z

Harry, G. J. (2013). Microglia during development and aging. *Pharmacology & Therapeutics*, *139*(3), 313–326. https://doi.org/10.1016/j.pharmthera.2013.04.013

Hasan, S., Foster, R. G., Vyazovskiy, V. V., & Peirson, S. N. (2018). Effects of circadian misalignment on sleep in mice. *Scientific Reports*, *8*(1), 15343. https://doi.org/10.1038/s41598-018-33480-1

Hastings, M. H., Reddy, A. B., & Maywood, E. S. (2003). A clockwork web: Circadian timing in brain and periphery, in health and disease. *Nature Reviews Neuroscience*, *4*(8), 649–661. https://doi.org/10.1038/nrn1177

Hayashi, Y. (2013). Diurnal Spatial Rearrangement of Microglial Processes through the Rhythmic Expression of P2Y12 Receptors. *Journal of Neurological Disorders*, *01*(02). https://doi.org/10.4172/2329-6895.1000120

Haynes, S. E., Hollopeter, G., Yang, G., Kurpius, D., Dailey, M. E., Gan, W.-B., & Julius, D. (2006). The P2Y12 receptor regulates microglial activation by extracellular nucleotides. *Nature Neuroscience*, *9*(12), 1512–1519. https://doi.org/10.1038/nn1805

Horsey, E. A., Maletta, T., Turner, H., Cole, C., Lehmann, H., & Fournier, N. M. (2020). Chronic Jet Lag Simulation Decreases Hippocampal Neurogenesis and Enhances Depressive Behaviors and Cognitive Deficits in Adult Male Rats. *Frontiers in Behavioral Neuroscience*, *13*, 272. https://doi.org/10.3389/fnbeh.2019.00272

Illes, P., Rubini, P., Ulrich, H., Zhao, Y., & Tang, Y. (2020). Regulation of Microglial Functions by Purinergic Mechanisms in the Healthy and Diseased CNS. *Cells*, *9*(5), 1108. https://doi.org/10.3390/cells9051108

Karatsoreos, I. N., Bhagat, S., Bloss, E. B., Morrison, J. H., & McEwen, B. S. (2011). Disruption of circadian clocks has ramifications for metabolism, brain, and behavior. *Proceedings of the National Academy of Sciences*, *108*(4), 1657–1662. https://doi.org/10.1073/pnas.1018375108

Kettenmann, H., Hanisch, U.-K., Noda, M., & Verkhratsky, A. (2011). Physiology of microglia. *Physiological Reviews*, *91*(2), 461–553. https://doi.org/10.1152/physrev.00011.2010

Knouse, M. C., McGrath, A. G., Deutschmann, A. U., Rich, M. T., Zallar, L. J., Rajadhyaksha, A. M., & Briand, L. A. (2022). Sex differences in the medial prefrontal cortical glutamate system. *Biology of Sex Differences*, *13*(1), 66. https://doi.org/10.1186/s13293-022-00468-6

Ko, C. H., & Takahashi, J. S. (2006). Molecular components of the mammalian circadian clock. *Human Molecular Genetics*, *15*(suppl_2), R271–R277. https://doi.org/10.1093/hmg/ddl207

Kono, R., Ikegaya, Y., & Koyama, R. (2021). Phagocytic Glial Cells in Brain Homeostasis. *Cells*, *10*(6), 1348. https://doi.org/10.3390/cells10061348

Leak, R. K., Card, J. P., & Moore, R. Y. (1999). Suprachiasmatic pacemaker organization analyzed by viral transynaptic transport. *Brain Research*, *819*(1–2), 23–32. https://doi.org/10.1016/s0006-8993(98)01317-1

Ma, X., Li, X., Wang, W., Zhang, M., Yang, B., & Miao, Z. (2022). Phosphatidylserine, inflammation, and central nervous system diseases. *Frontiers in Aging Neuroscience*, *14*. https://doi.org/10.3389/fnagi.2022.975176

Madry, C., & Attwell, D. (2015). Receptors, Ion Channels, and Signaling Mechanisms Underlying Microglial Dynamics *. *Journal of Biological Chemistry*, *290*(20), 12443–12450. https://doi.org/10.1074/jbc.R115.637157

Magistretti, P. J., & Allaman, I. (2015). A Cellular Perspective on Brain Energy Metabolism and Functional Imaging. *Neuron*, *86*(4), 883–901. https://doi.org/10.1016/j.neuron.2015.03.035

Masuda, T., Sankowski, R., Staszewski, O., & Prinz, M. (2020). Microglia Heterogeneity in the Single-Cell Era. *Cell Reports*, *30*(5), 1271–1281. https://doi.org/10.1016/j.celrep.2020.01.010

Meng, D., Yang, M., Zhang, H., Zhang, L., Song, H., Liu, Y., Zeng, Y., Yang, B., Wang, X., Chen, Y., & Liu, R. (2023). Microglia activation mediates circadian rhythm disruption-induced cognitive impairment in mice. *Journal of Neuroimmunology*, *379*, 578102. https://doi.org/10.1016/j.jneuroim.2023.578102

Miller, J. D., Morin, L. P., Schwartz, W. J., & Moore, R. Y. (1996). New Insights Into the Mammalian Circadian Clock. *Sleep*, *19*(8), 641–667. https://doi.org/10.1093/sleep/19.8.641

Nimmerjahn, A., Kirchhoff, F., & Helmchen, F. (2005). Resting Microglial Cells Are Highly Dynamic Surveillants of Brain Parenchyma in Vivo. *Science*, *308*(5726), 1314–1318. https://doi.org/10.1126/science.1110647

Ohsawa, K., Imai, Y., Kanazawa, H., Sasaki, Y., & Kohsaka, S. (2000). Involvement of Iba1 in membrane ruffling and phagocytosis of macrophages/microglia. *Journal of Cell Science*, *113*(17), 3073–3084. https://doi.org/10.1242/jcs.113.17.3073

Paolicelli, R. C., Bolasco, G., Pagani, F., Maggi, L., Scianni, M., Panzanelli, P., Giustetto, M., Ferreira, T. A., Guiducci, E., Dumas, L., Ragozzino, D., & Gross, C. T. (2011). Synaptic Pruning by Microglia Is Necessary for Normal Brain Development. *Science*, *333*(6048), 1456–1458. https://doi.org/10.1126/science.1202529

Patton, A. P., & Hastings, M. H. (2018). The suprachiasmatic nucleus. *Current Biology*, *28*(15), R816–R822. https://doi.org/10.1016/j.cub.2018.06.052

Pawelec, P., Ziemka-Nalecz, M., Sypecka, J., & Zalewska, T. (2020). The Impact of the CX3CL1/CX3CR1 Axis in Neurological Disorders. *Cells*, *9*(10), 2277. https://doi.org/10.3390/cells9102277

Phillips, D. J., Savenkova, M. I., & Karatsoreos, I. N. (2015). Environmental disruption of the circadian clock leads to altered sleep and immune responses in mouse. *Brain, Behavior, and Immunity*, *47*, 14–23. https://doi.org/10.1016/j.bbi.2014.12.008

Reddaway, J., Richardson, P. E., Bevan, R. J., Stoneman, J., & Palombo, M. (2023). Microglial morphometric analysis: So many options, so little consistency. *Frontiers in Neuroinformatics*, *17*, 1211188. https://doi.org/10.3389/fninf.2023.1211188

Roberts, B. L., & Karatsoreos, I. N. (2023). Circadian desynchronization disrupts physiological rhythms of prefrontal cortex pyramidal neurons in mice. *Scientific Reports*, *13*(1), 9181. https://doi.org/10.1038/s41598-023-35898-8

Ruan, C., & Elyaman, W. (2022). A New Understanding of TMEM119 as a Marker of Microglia. *Frontiers in Cellular Neuroscience*, *16*, 902372. https://doi.org/10.3389/fncel.2022.902372

Sato, M., Chang, E., Igarashi, T., & Noble, L. J. (2001). Neuronal injury and loss after traumatic brain injury: Time course and regional variability. *Brain Research*, *917*(1), 45–54. https://doi.org/10.1016/S0006-8993(01)02905-5

Scharfman, H. E. (2007). The neurobiology of epilepsy. *Current Neurology and Neuroscience Reports*, *7*(4), 348–354. https://doi.org/10.1007/s11910-007-0053-z

Siddique, R., Awan, F. M., Nabi, G., Khan, S., & Xue, M. (2022). Chronic jet lag-like conditions dysregulate molecular profiles of neurological disorders in nucleus accumbens and prefrontal cortex. *Frontiers in Neuroinformatics*, *16*. https://doi.org/10.3389/fninf.2022.1031448

Sierra, A., Abiega, O., Shahraz, A., & Neumann, H. (2013). Janus-faced microglia: Beneficial and detrimental consequences of microglial phagocytosis. *Frontiers in Cellular Neuroscience*, *7*. https://doi.org/10.3389/fncel.2013.00006

Smolders, S. M.-T., Kessels, S., Vangansewinkel, T., Rigo, J.-M., Legendre, P., & Brône, B. (2019). Microglia: Brain cells on the move. *Progress in Neurobiology*, *178*, 101612. https://doi.org/10.1016/j.pneurobio.2019.04.001

Stephan, F. K., & Zucker, I. (1972). Circadian Rhythms in Drinking Behavior and Locomotor Activity of Rats Are Eliminated by Hypothalamic Lesions. *Proceedings of the National Academy of Sciences*, *69*(6), 1583–1586. https://doi.org/10.1073/pnas.69.6.1583

Stillman, J. M., Mendes Lopes, F., Lin, J.-P., Hu, K., Reich, D. S., & Schafer, D. P. (2023). Lipofuscin-like autofluorescence within microglia and its impact on studying microglial engulfment. *Nature Communications*, *14*(1), 7060. https://doi.org/10.1038/s41467-023-42809-y

Sun, Y., Ip, P., & Chakrabartty, A. (2017). Simple Elimination of Background Fluorescence in Formalin-Fixed Human Brain Tissue for Immunofluorescence Microscopy. *Journal of Visualized Experiments: JoVE*, *127*, 56188. https://doi.org/10.3791/56188

Tay, T. L., Mai, D., Dautzenberg, J., Fernández-Klett, F., Lin, G., Sagar, Datta, M., Drougard, A., Stempfl, T., Ardura-Fabregat, A., Staszewski, O., Margineanu, A., Sporbert, A., Steinmetz, L. M., Pospisilik, J. A., Jung, S., Priller, J., Grün, D., Ronneberger, O., & Prinz, M. (2017). A new fate mapping system reveals context-dependent random or clonal expansion of microglia. *Nature Neuroscience*, *20*(6), 793–803. https://doi.org/10.1038/nn.4547

Taylor, S. E., Morganti-Kossmann, C., Lifshitz, J., & Ziebell, J. M. (2014). Rod Microglia: A Morphological Definition. *PLoS ONE*, *9*(5), e97096. https://doi.org/10.1371/journal.pone.0097096

Turek, F. W., Joshu, C., Kohsaka, A., Lin, E., Ivanova, G., McDearmon, E., Laposky, A., Losee-Olson, S., Easton, A., Jensen, D. R., Eckel, R. H., Takahashi, J. S., & Bass, J. (2005). Obesity and metabolic syndrome in circadian Clock mutant mice. *Science (New York, N.Y.)*, *308*(5724), 1043–1045. https://doi.org/10.1126/science.1108750

Vetter, C. (2020). Circadian disruption: What do we actually mean? *European Journal of Neuroscience*, *51*(1), 531–550. https://doi.org/10.1111/ejn.14255

Vidal-Itriago, A., Radford, R. A. W., Aramideh, J. A., Maurel, C., Scherer, N. M., Don, E. K., Lee, A., Chung, R. S., Graeber, M. B., & Morsch, M. (2022). Microglia morphophysiological diversity and its implications for the CNS. *Frontiers in Immunology*, *13*. https://www.frontiersin.org/articles/10.3389/fimmu.2022.997786

Wake, H., Moorhouse, A. J., Jinno, S., Kohsaka, S., & Nabekura, J. (2009). Resting Microglia Directly Monitor the Functional State of Synapses In Vivo and Determine the Fate of Ischemic Terminals. *Journal of Neuroscience*, *29*(13), 3974–3980. https://doi.org/10.1523/JNEUROSCI.4363-08.2009

Walker, W. H., Walton, J. C., DeVries, A. C., & Nelson, R. J. (2020). Circadian rhythm disruption and mental health. *Translational Psychiatry*, *10*(1), 1–13. https://doi.org/10.1038/s41398-020-0694-0

Wang, K., Li, J., Zhang, Y., Huang, Y., Chen, D., Shi, Z., Smith, A. D., Li, W., & Gao, Y. (2021). Central nervous system diseases related to pathological microglial phagocytosis. *CNS Neuroscience & Therapeutics*, *27*(5), 528–539. https://doi.org/10.1111/cns.13619

Weinhard, L., di Bartolomei, G., Bolasco, G., Machado, P., Schieber, N. L., Neniskyte, U., Exiga, M., Vadisiute, A., Raggioli, A., Schertel, A., Schwab, Y., & Gross, C. T. (2018). Microglia remodel synapses by presynaptic trogocytosis and spine head filopodia induction. *Nature Communications*, *9*(1), 1228. https://doi.org/10.1038/s41467-018-03566-5

Wright, K. P. J., Lowry, C. A., & LeBourgeois, M. K. (2012). Circadian and wakefulness-sleep modulation of cognition in humans. *Frontiers in Molecular Neuroscience*, *5*. https://doi.org/10.3389/fnmol.2012.00050

Yan, L., Karatsoreos, I., LeSauter, J., Welsh, D. K., Kay, S., Foley, D., & Silver, R. (2007). Exploring Spatiotemporal Organization of SCN Circuits. *Cold Spring Harbor Symposia on Quantitative Biology*, *72*, 527–541. https://doi.org/10.1101/sqb.2007.72.037

Yang, C., & Wang, X. (2021). Lysosome biogenesis: Regulation and functions. *Journal of Cell Biology*, *220*(6), e202102001. https://doi.org/10.1083/jcb.202102001

Yang, I., Han, S. J., Kaur, G., Crane, C., & Parsa, A. T. (2010). The Role of Microglia in Central Nervous System Immunity and Glioma Immunology. *Journal of Clinical Neuroscience : Official Journal of the Neurosurgical Society of Australasia*, *17*(1), 6–10. https://doi.org/10.1016/j.jocn.2009.05.006

Yanguas-Casás, N., Crespo-Castrillo, A., de Ceballos, M. L., Chowen, J. A., Azcoitia, I., Arevalo, M. A., & Garcia-Segura, L. M. (2018). Sex differences in the phagocytic and migratory activity of microglia and their impairment by palmitic acid. *Glia*, *66*(3), 522–537. https://doi.org/10.1002/glia.23263

Yilmaz, M., Yalcin, E., Presumey, J., Aw, E., Ma, M., Whelan, C. W., Stevens, B., McCarroll, S. A., & Carroll, M. C. (2021). Overexpression of schizophrenia susceptibility factor human complement C4A promotes excessive synaptic loss and behavioral changes in mice. *Nature Neuroscience*, *24*(2), 214–224. https://doi.org/10.1038/s41593-020-00763-8